

In vitro evolution of an L-amino acid deaminase active on L-1-naphthylalanine

Roberta Melis, Elena Rosini, Valentina Pirillo, Loredano Pollegioni, Gianluca Molla

Dipartimento di Biotecnologie e Scienze della Vita, Università degli Studi dell'Insubria, via J. H.

Dunant 3, 21100 Varese, Italy.

Supplementary Materials:

Table S1 Analysis of the genetic diversity of the libraries of PmaLAAD variants generated by site-saturation mutagenesis.

Position	Original codon	Number of sequenced clones	Introduced mutation	Encoded residue	Fraction of variants (%)
First-generation, single-site PmaLAAD variants (template gene: <i>PmaLAAD-00N</i>)					
L279	TTA	6	GGG TTG GTT GGT GGG ATG	Gly Leu Val Gly Gly Met	100
F318	TTC	6	GGG ACT CCT TTG TTT TGG	Gly Thr Pro Leu Phe Trp	100
V412	GTA	7	CTT GCG GTT GTT GTA* AGG GGG	Leu Ala Val Val Val Arg Gly	86
V438	GTG	6	CCG GCG GAT TCG GGG CAT	Pro Ala Asp Ser Gly His	100

W439	TGG	7	TAT CTG CAG CTG TAT CGG AGT	Tyr Leu Leu Leu Tyr Arg Ser	100
First-generation, double-site PmaLAAD variants (template gene: <i>PmaLAAD-00N</i>)					
S99/Q100	AGC/CAA	10	TAT/TGT ATT/CAT CTT/AAT TTT/TGT TTT/AGT TAT/CGT CAT/CAT TGT/CAT CAT/AAT GTT/CTT CAT/GTA*	Tyr/Cys Ile/His Leu/Asn Phe/Cys Phe/Ser Tyr/Arg His/His Cys/His His/Asn Val/Leu His/Val	100
F318/V412	TTC/GTA	10	TAT/GGT TAT/ATT TAT/ATT TAT/TGT CGT/TGT AAT/TAT TGT/ATT TTT/GAT AAT/AAT	Tyr/Gly Tyr/Ile Tyr/Ile Tyr/Cys Arg/Cys Asn/Tyr Cys/Ile Phe/Asp Asn/Asn	100
Second-generation PmaLAAD variants (template gene: V412A/V438P-<i>PmaLAAD-00N</i>)					
L279	TTA	10	CGG TTA* AGG GAT GTG CTT TCT CCG AGT CGT	Arg Leu Lys Asp Val Leu Ser Pro Ser Arg	90
F318	TTC	12	CAG ATT CGT TGG GTT TGG CAT TTT GAT TGG CCG TTC*	Gln Ile Arg Trp Val Trp His Phe Asp Trp Pro Phe	91.7

*parental DNA

Table S2 Expression and purification of wild-type PmaLAAD and variants. Proteins were purified from cells harvested from 1 L of culture. Activity values were determined on 50 mM L-Phe as substrate. (BD: below detection; ND: not determined).

Variant	Specific activity (U/mg)	Protein yield	
		mg/g cells	mg/L culture
Wild-type	2.90	1.0	9.9
First-generation, single-site variants (template gene: <i>PmaLAAD-00N</i>)			
L279G	0.35	0.4	4.4
F318A	1.36	0.7	4.0
F318C ¹	0.90	0.5	3.5
F318G ¹	0.97	0.7	5.0
F318I ¹	1.34	1.7	8.9
F318L	0.89	0.5	4.7
F318M	1.04	0.7	5.8
F318V	0.39	0.7	6.4
V412A	2.85	0.6	5.9
V412L	2.99	0.8	6.2
V412A/V438P	0.63	0.8	6.1
V438G	0.45	0.6	4.8
V438P	1.14	1.1	6.4
First-generation, double-site variants (template gene: <i>PmaLAAD-00N</i>)			
F318C/V412L	0.82	0.4	3.5
F318C/V412G	0.07	0.5	3.1
F318G/V412G	BD	0.5	3.0
F318I/V412S	0.48	0.7	7.8
F318S/V412S	0.12	0.4	4.2
F318V/V412L ²	ND	ND	ND
F318V/V412G	0.32	1.1	6.9
F318V/V412I	1.45	0.2	1.6
F318V/V412S	0.79	0.1	1.0
Second-generation variants (template gene: <i>V412A/V438P PmaLAAD-00N</i>)			
F318A/V412A/V438P	0.63	1.0	6.7

¹These variants were identified in the second round of SSM.

² This variant was purified as apoprotein.

Table S3 Apparent kinetic parameters of selected PmaLAAD variants on L-Phe and L-1-Nal.

	L-Phe					L-1-Nal				Specificity constant
	V_{max} (U/mg)	k_{cat} (s ⁻¹)	K_m (mM)	K_i (mM)	k_{cat}/K_m (s ⁻¹ mM ⁻¹)	V_{max} (U/mg)	k_{cat} (s ⁻¹)	K_m (mM)	k_{cat}/K_m (s ⁻¹ mM ⁻¹)	$(k_{cat}/K_m)_{L-1-Nal} / (k_{cat}/K_m)_{L-Phe}$
Wild-type	3.00 ± 0.04	2.66 ± 0.04	1.60 ± 0.09	-	1.66 ± 0.12	1.18 ± 0.24 ¹	1.05 ± 0.21	0.79 ± 0.02 ¹	1.30 ± 0.29	0.78 ± 0.25
First-generation, single-site variants (template gene: <i>PmaLAAD-00N</i>)										
L279G	0.67 ± 0.17	0.59 ± 0.15	40 ± 19	-	0.01 ± 0.01	BD			-	-
F318A	1.53 ± 0.1	1.36 ± 0.09	3.76 ± 0.98	-	0.36 ± 0.12	1.15 ± 0.06	1.02 ± 0.05	0.24 ± 0.03	4.3 ± 0.8	11.9 ± 2.4
F318C¹	1.04 ± 0.07	0.92 ± 0.06	5.7 ± 1.5	-	0.16 ± 0.05	0.65 ± 0.02	0.58 ± 0.02	0.35 ± 0.03	1.7 ± 0.2	10.6 ± 1.6
F318G¹	1.32 ± 0.23	1.17 ± 0.20	1.87 ± 0.94	-	0.63 ± 0.42	0.98 ± 0.09	0.87 ± 0.08	0.21 ± 0.04	4.1 ± 1.2	6.5 ± 2.5
F318I3¹	1.44 ± 0.03	1.28 ± 0.03	1.8 ± 0.2	-	0.71 ± 0.09	1.10 ± 0.10	0.96 ± 0.09	0.31 ± 0.06	3.1 ± 0.9	4.4 ± 1.4
F318L	0.94 ± 0.02	0.83 ± 0.02	0.98 ± 0.10	-	0.85 ± 0.11	0.85 ± 0.06	0.75 ± 0.05	0.16 ± 0.03	4.7 ± 1.2	5.5 ± 1.52
F318M	1.09 ± 0.02	0.97 ± 0.02	1.05 ± 0.09	-	0.92 ± 0.1	1.10 ± 0.06	0.98 ± 0.05	0.41 ± 0.04	2.4 ± 0.4	2.6 ± 0.5
F318V	0.19 ± 0.01	0.17 ± 0.01	5.95 ± 1.02	-	0.03 ± 0.01	0.13 ± 0.02	0.12 ± 0.02	0.13 ± 0.05	0.9 ± 0.5	30 ± 17
V412A	3.04 ± 0.07	2.7 ± 0.06	2.75 ± 0.26	-	0.98 ± 0.11	1.33 ± 0.17 ²	1.18 ± 0.15	0.61 ± 0.13 ²	1.9 ± 0.7	1.9 ± 0.7
V412A-V438P	1.59 ± 0.4	1.41 ± 0.35	7.4 ± 2.6	23.5 ± 7.7	0.19 ± 0.11	1.74 ± 0.29	1.55 ± 0.26	0.52 ± 0.10	3.1 ± 1.1	15.8 ± 6.2
V438G	1.53 ± 0.21	1.36 ± 0.19	3.94 ± 0.99	14.2 ± 3.5	0.35 ± 0.14	0.84 ± 0.08	0.75 ± 0.07	0.5 ± 0.09	1.5 ± 0.4	4.3 ± 1.6
V438P	2.34 ± 0.05	2.08 ± 0.04	1.64 ± 0.08	47.6 ± 2.8	1.27 ± 0.09	1.71 ± 0.23 ²	1.52 ± 0.21	1.28 ± 0.25 ²	1.2 ± 0.4	0.9 ± 0.4
First-generation, double-site variants (template gene: <i>PmaLAAD-00N</i>)										
F318V/V412G	1.02 ± 0.1	0.90 ± 0.09	7.2 ± 1.2	24.8 ± 3.8	0.12 ± 0.03	1.51 ± 0.02	1.34 ± 0.02	0.27 ± 0.01	5.0 ± 0.26	41.7 ± 2.4
F318I/V412S	0.56 ± 0.03	0.50 ± 0.03	1.77 ± 0.48	-	0.28 ± 0.09	0.76 ± 0.07	0.67 ± 0.06	0.08 ± 0.02	8.4 ± 2.9	30 ± 10.5
F318C/V412L	0.99 ± 0.02	0.88 ± 0.02	9.9 ± 0.7	-	0.09 ± 0.01	0.58 ± 0.06	0.51 ± 0.05	0.67 ± 0.12	0.8 ± 0.2	8.9 ± 2.6
F318C/V412G	0.17 ± 0.01	0.15 ± 0.01	0.77 ± 0.09	32.9 ± 3.7	0.19 ± 0.03	0.39 ± 0.02	0.35 ± 0.02	0.15 ± 0.02	2.3 ± 0.44	12.1 ± 2.5
F318V/V412S	0.97 ± 0.15	0.86 ± 0.13	13.4 ± 5.4	-	0.06 ± 0.03	1.54 ± 0.3 ²	1.37 ± 0.28	0.58 ± 0.13 ²	2.4 ± 1.04	40 ± 18

F318V/V412I	1.64 ± 0.07	1.45 ± 0.06	7.8 ± 1.1	-	0.19 ± 0.04					BD
Second-generation variants (template gene: V412A/V438P-<i>PmaLAAD-00N</i>)										
F318A/V412A/V438P	0.71 ± 0.02	0.63 ± 0.02	6.0 ± 0.9	-	0.11 ± 0.02	1.77 ± 0.05	1.57 ± 0.04	0.17 ± 0.01	9.2 ± 0.8	83.6 ± 7.3

¹These variants were identified in the first-generation, double-site, SSM.

² Values estimated using the Lineweaver-Burk plot.

Table S4. Primers used for site-saturation mutagenesis carrying the NNK or NDT degenerated codon.

Position	Primers with NNK codon
L279	Forward: 5'-CCAACCTGAATGTTTACNNKTCACAACAACGTGTATC-3' Reverse: 5'-GATACACGTTGTTGTGAMNNGTAAACATTCAAGGTTGG-3'
F318	Forward: 5'-CTTATGCTGTAGCCCCACGTATCNNKACAAGCTCCATTG-3' Reverse: 5'-CAATGGAGCTTGTMMNNGATACGTGGGGCTACAGCATAAG-3'
V412	Forward: 5'-GAACGTTGGGGTGCAGTTNNKAGTCCAACATTTGATG-3' Reverse: 5'-CATCAAATGTTGGACTMNNAACTGCACCCCAACGTTC 3'
V438	Forward: 5'-CAATACAGCGACANNKTGGGGAATGACAGAAGGTCC-3' Reverse: 5'-GGACCTTCTGTCATTCCCCAMNNTGTCGCTGTATTG-3'
W439	Forward: 5'-CAATACAGCGACAGTGNNKGGGAATGACAGAAGGTCC-3' Reverse: 5'-GGACCTTCTGTCATTCCMNNCACTGTCGCTGTATTG-3'
Position	Primers with NDT codon
F318	Forward: 5'-CTTATGCTGTAGCCCCACGTATCNDTACAAGCTCCATTG-3' Reverse: 5'-CAATGGAGCTTGTAAHNGATACGTGGGGCTACAGCATAAG-3'
V412	Forward: 5'-GAACGTTGGGGTGCAGTTNDTAGTCCAACATTTGATG-3' Reverse: 5'-CATCAAATGTTGGACTAHNAACTGCACCCCAACGTTC-3'
S99/Q100	Forward: 5'-GAGCAATCAGGCCGCGCATAACNDTNDTATCATTAGCTACCAAACGTC-3' Reverse: 5'-GACGTTTGGTAGCTAATGATAHNAHNGTATGCGCGCCTGATTGCTC-3'

Figure S1

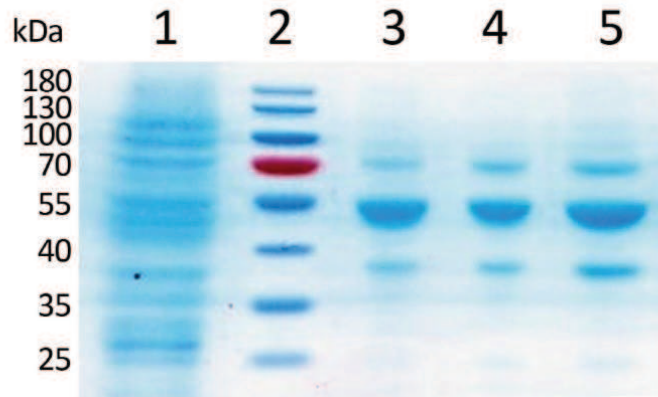


Figure S1 SDS-PAGE analysis of selected purified PmaLAAD variants. Lane 1: crude extract (80 μ g); lane 2: LMW markers (Prestained Protein Ladder, PageRuler™); lane 3: wild-type PmaLAAD; lane 4: V412A/V438P variant; lane 5: F318A/V412A/V438P variant. For each lane 5 μ g of total proteins were loaded.

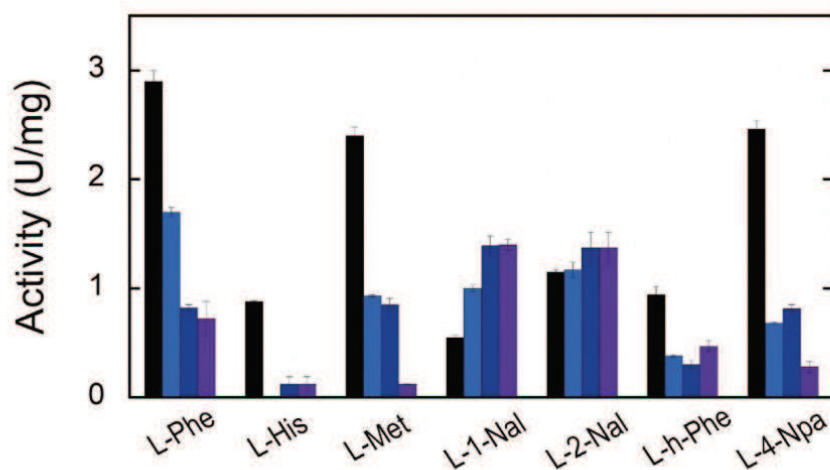


Figure S2

Figure S2 Substrate scope (reported as specific activity) of wild-type (black), F318A (cyan), V412A/V438P (blue), and F318A/V412A/V438P (purple) PmaLAAD variants. The enzymatic activity was measured using the polarographic assay. The enzymatic activity was determined on different natural and synthetic L-amino acids: 50 mM L-Phe, 50 mM L-His, 50 mM L-Met, 1.2 mM D,L-1-naphthylalanine (D,L-1-Nal), 1.2 mM D,L-2-naphthylalanine (D,L-2-Nal), 0.7 mM D,L-1-naphthylglycine (D,L-1-NGly), 0.7 mM D,L-2-naphthylglycine (D,L-2-NGly), 5 mM D,L-homophenylalanine (D,L-h-Phe), and 10 mM L-4-nitrophenylalanine (L-4-Npa) under standard conditions (50 mM potassium phosphate, pH 7.5, 25 °C and at air saturation).

Figure S3

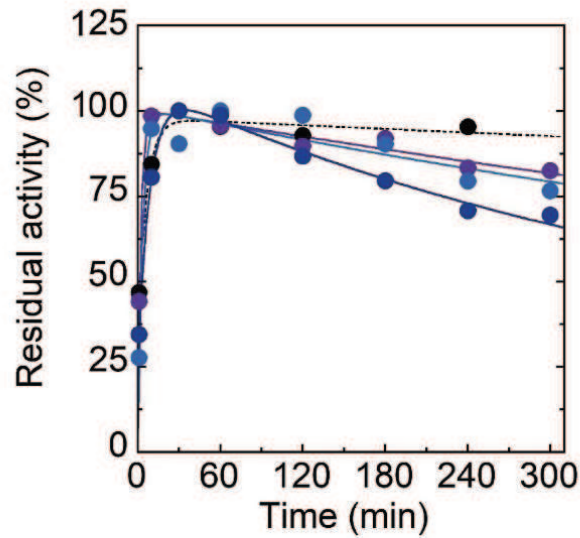


Figure S3 Time course of enzymatic activity of wild-type PmaLAAD and selected variants at 25 °C in presence of *E. coli* membranes added before starting the experiment. Wild-type PmaLAAD, $k_{\text{fast}} = 9.09 \pm 1.65 \text{ min}^{-1}$, $k_{\text{slow}} = 0.018 \pm 0.004$ (black); F318A, $k_{\text{fast}} = 17.3 \pm 9.8$, $k_{\text{slow}} = 0.06 \pm 0.05 \text{ min}^{-1}$ (cyan); V412A/V438P, $k_{\text{fast}} = 7.0 \pm 0.7 \text{ min}^{-1}$, $k_{\text{slow}} = 0.14 \pm 0.01 \text{ min}^{-1}$ (blue); V412A/V438P/F318A, $k_{\text{fast}} = 25.1 \pm 16.3 \text{ min}^{-1}$, $k_{\text{slow}} = 0.04 \pm 0.02 \text{ min}^{-1}$ (purple). We defined k_{fast} as the rate of PmaLAAD reactivation following membrane addition and k_{slow} as the rate of PmaLAAD inactivation during the subsequent incubation at 25 °C.

Figure S4

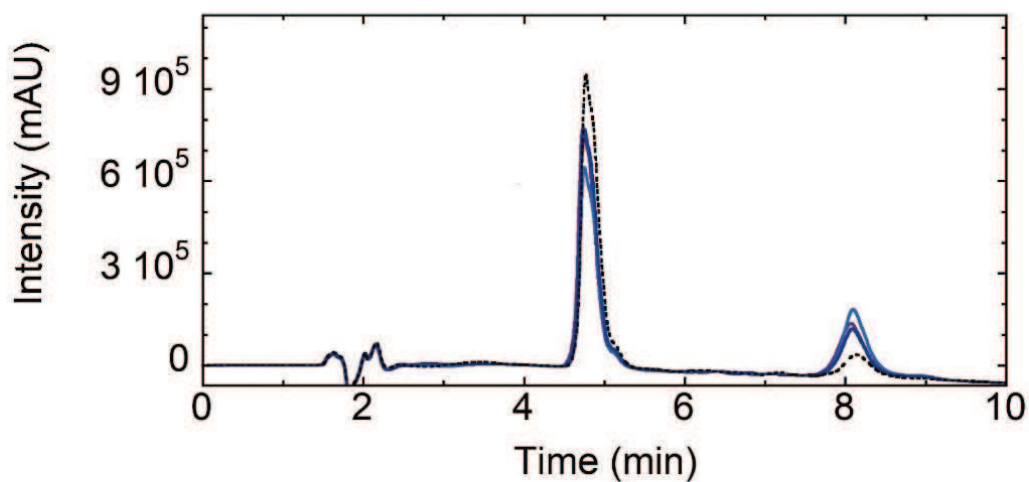


Figure S4. HPLC chromatograms after 10 min of bioconversion of D,L-1-Nal (retention time = 4.7 min) to 1-naphthylpyruvate (retention time = 8.1 min) catalyzed by wild-type PmaLAAD (dashed line) or the F318A (cyan), V412A/V438P (blue), and F318A/V412A/V438P (purple). Conditions: 1.2 mM substrate, 0.05 mg/mL PmaLAAD-00N or different PmaLAAD variants, *E. coli* membranes, pH 7.5, 25 °C (1.0 mL).

Optimization of F318A/V412A/V438P PmaLAAD expression

Optimization of expression conditions

Starter cultures were prepared by growing a single colony of *E. coli* BL21(DE3) cells carrying the recombinant pET11a-PmaLAAD-00N or pET11a-PmaLAAD-F318A/V412A/V438P plasmid overnight at 37 °C in flasks containing TB broth to which 100 µg/mL ampicillin was added. These cultures were diluted with the same media to a starting OD_{600nm} of 0.1 and then incubated at 37 °C on a rotatory shaker at 200 rpm. Experiments were carried out in 500 mL baffled Erlenmeyer flasks containing 125 mL of liquid media at 37 °C and 200 rpm. Both the optical density and the pH value of the medium were assayed every hour. Growth curves were generated by the interpolation of OD_{600nm} values according to the Gompertz equation (Zwietering et al., 1990).

In order to optimize F318A/V412A/V438P PmaLAAD production in *E. coli* BL21(DE3) cells, the effect of adding 0.1 mM IPTG at different phases of the growth curve (corresponding to OD₆₀₀ of 0.5, 2, 5), of the temperature of growth (28 or 15 °C), and of the time of cell harvest (4 h or overnight after IPTG addition) on protein expression was investigated. The LAAD enzymatic activity of crude extracts (50 µL) was determined by using the polarographic assay (see below) on 1.2 mM D,L-1-Nal. Since the F318A/V412A/V438P PmaLAAD showed the most interesting enzymatic properties, the expression conditions of this recombinant enzyme in BL21(DE3) *E. coli* cells were optimized using a *semi*-factorial design approach. The growth curve of the variant was almost superimposable to the one of the PmaLAAD-00N wild-type with almost identical Gompertz equation parameters (Figure S5a). The temperature, induction growth phase, and the interval between IPTG addition and cell harvesting were evaluated. The best expression condition was: adding 0.1 mM IPTG at OD_{600nm} = 2.0 (corresponding to a mid-exponential growth phase) and collecting cells after overnight growth at 28 °C (condition 4). Under these conditions, a 4.5-fold higher volumetric yield (235 U/L) was reached than the one obtained under standard conditions (i.e., induction at OD_{600nm} = 0.5 and collecting cells

melis.supplementary-edited.180917.docx

after 4 hours at 28 °C). This result is due to a 2-fold increase in enzyme activity value per gram of cells and of the biomass accumulation (Table S5 and Figure S5b).

M.H. Zwietering, I. Jongenburger, F.M. Rombouts, and K. Van't Riet, *App. Env. Microbiol.*, 1990, **56**, 1875-1881.

Table S5

Conditions tested for the recombinant expression of F318A/V412A/V438P PmaLAAD variant.

Conditions	g of cells
1; OD _{600 nm} = 0.5, 28 °C, harvest time = 4 h	1.15
2; OD _{600 nm} = 0.5, 28 °C, harvest time = overnight	2.52
3; OD _{600 nm} = 2, 28 °C, harvest time = 4 h	2.04
4; OD _{600 nm} = 2, 28 °C, harvest time = overnight	2.18
5; OD _{600 nm} = 5, 28 °C, harvest time = 4 h	2.26
6; OD _{600 nm} = 5, 28 °C, harvest time = overnight	2.73
7; OD _{600 nm} = 0.5, 15 °C, harvest time = 4 h	0.41
8; OD _{600 nm} = 0.5, 15 °C, harvest time = overnight	2.06
9; OD _{600 nm} = 2, 15 °C, harvest time = 4 h	1.09
10; OD _{600 nm} = 2, 28 °C, harvest time = overnight	2.32
11; OD _{600 nm} = 5, 15 °C, harvest time = 4 h	1.99
12; OD _{600 nm} = 5, 15 °C, harvest time = overnight	2.66

Experiments were carried out in 500 mL baffled Erlenmeyer flasks containing 125 mL of TB broth.

Figure S5

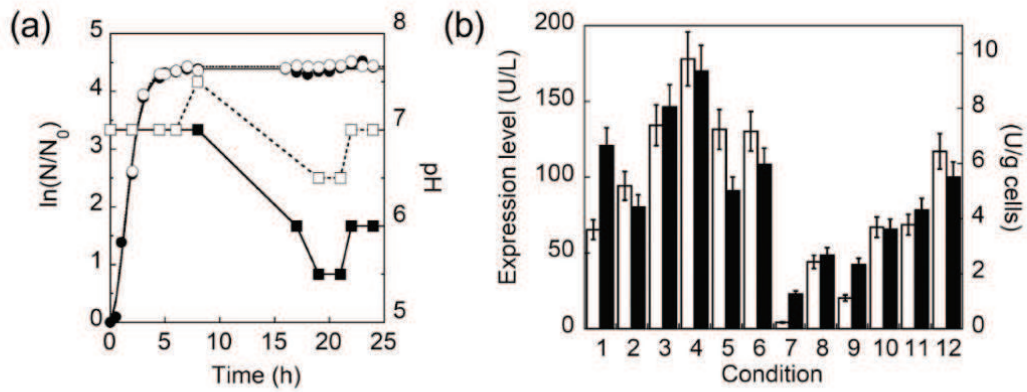


Figure S5: (a) Growth curve of BL21(DE3) *E. coli* cells carrying the pET11b-PmaLAAD-00N (○) or the pET11b-PmaLAAD-F318A/V412A/V438P (◻) plasmid in Terrific broth. pH of the growing medium (PmaLAAD-00N, ○; F318A/V412A/V438P variant, ●). (b) Expression yields of F318A/V412A/V438P PmaLAAD under different conditions (conditions reported in Table S5). The activity values were determined under standard conditions on 1.2 mM D,L-1-Nal as a substrate (i.e. in the presence of *E. coli* membranes at pH 7.5, 25 °C).

3.2.2 Screening of PmaLAAD variants (obtained by site-saturation mutagenesis) on different substrates of biotechnological interest

We took advantage from the availability of the libraries of PmaLAAD variants produced in *Melis et al., 2018*¹, to screen for novel variants active on substrates of biotechnological relevance. These substrates were L-amino acids (both natural and synthetic), whose D-enantiomer is used as building block for the synthesis of high-value compounds such as drugs or food additives.

Results

Variants were screened by the colorimetric assay on several substrates of biotechnological interest (L-amino acids). The LAAD activity was assayed on the crude extract by adding 50 μ L of substrate solutions following the procedures described in *Melis et al., 2018*¹. In the first-generation of mutagenesis, LAAD activity was assayed on 50 mM L-Phe, 50 mM L-Leu, 50 mM L-His, 50 mM L-Asp, 50 mM L-Ser, 1.2 mM D,L-1-Nala, 0.75 mM D,L-naphthyl-Gly, 50 mM L-dihydroxyPhe or 50 mM D,L-tert-Leu in 50 mM potassium phosphate buffer, pH 7.5, while in the second generation of mutagenesis it was assayed on 50 mM L-Phe, 50 mM L-Met, 50 mM L-Leu, 50 mM L-His, 50 mM L-Asp, 10 mM L-4-nitro-Phe, 1.2 mM D,L-1-Nala, 5 mM methoxy-PheGly, 50 mM L-penicillamine or 50 mM D, L-tert-Leu in 50 mM potassium phosphate buffer, pH 7.5.

Unfortunately, no variants showed a significant improved activity on these substrates with the exception of V412L-PmaLAAD, which showed an increased activity on the reference substrate L-Phe and on L-Leu in comparison to the wild-type; the relative activity was 145% on L-Phe, 148% on L-Leu and 113% on D,L-1-Nal. This variant was expressed in *E. coli* and purified by metal chelating affinity chromatography following the conditions used for the wild-type protein². The volumetric yield was comparable to the wild-type. Recombinant V412L-PmaLAAD variant migrates as a single band at \approx 51 kDa in SDS-PAGE, with >

80% purity (Fig. 1). The expression and purification yield are reported in Table 1. The pure V412L-PmaLAAD shows the same specific activity of the wild-type enzyme on L-Phe (Tab. 1).

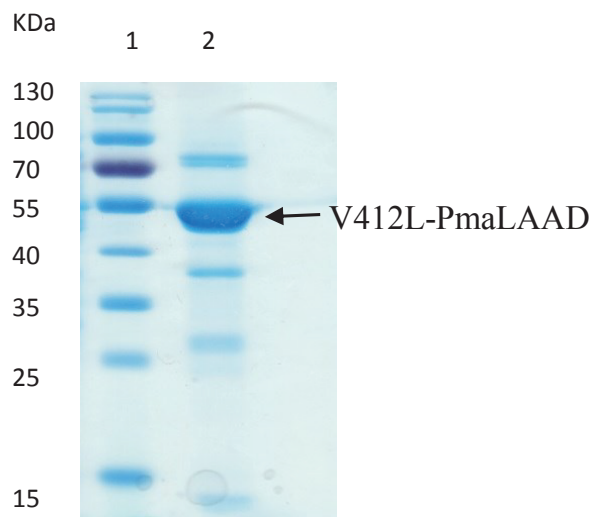


Figure 1. SDS-PAGE analysis of purified V412L-PmaLAAD variant. Lane 1: LMW markers (Prestained Protein Ladder, PageRuler™); lane 2: 5 μ g of pure V412L-PmaLAAD.

Table 1. Expression and purification of V412L-PmaLAAD. Wild-type and V412L-PmaLAAD variant were purified from cells harvested from 1 L of culture. Activity values were determined on 50 mM L-Phe as substrate.

Variant	Specific activity	Protein yield	
	(U/mg)	mg/g cells	mg/L culture
Wild-type	2.90	1.0	9.9
V412L	2.99	0.8	6.2

The apparent kinetic parameters of the purified V412L-PmaLAAD was determined in the presence of *E. coli* membranes at pH 7.5, 25 °C on L-Phe (the reference substrate) and L-Leu (Fig. 2, Tab. 2).

Table 2. Apparent kinetic parameters on L-Phe and L-Leu of wild-type and V412L-PmaLAAD variant.

Variant	L-Phe			L-Leu		
	V_{\max} (U/mg)	K_m (mM)	V_{\max}/K_m	V_{\max} (U/mg)	K_m (mM)	V_{\max}/K_m
Wild-type	3.00 ± 0.04	1.60 ± 0.09	1.88	2.73 ± 0.02	0.46 ± 0.02	5.93
V412L	3.46 ± 0.02	7.88 ± 0.14	0.44	3.03 ± 0.02	4.78 ± 0.13	0.63

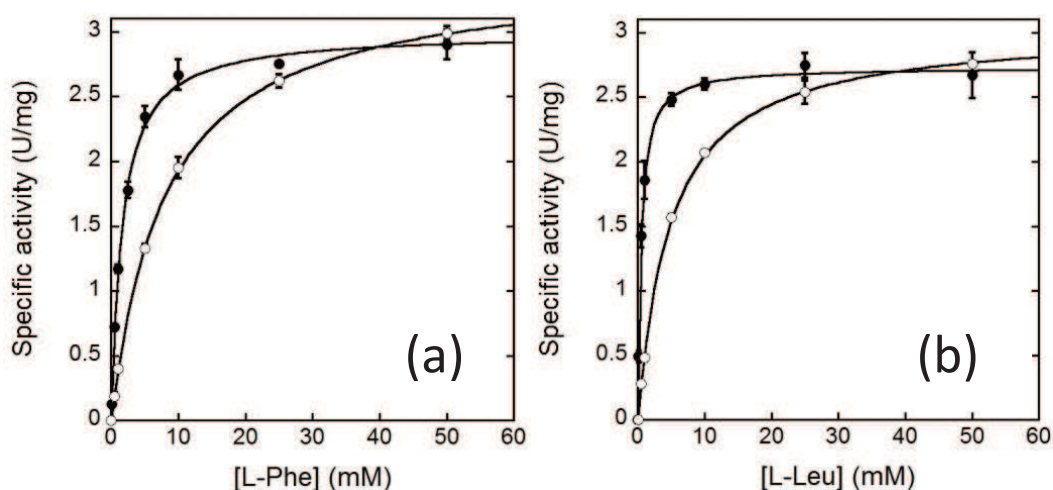


Figure 2. Determination of apparent kinetic parameters of wild-type (black) and V412L-PmaLAAD (open circles) on L-Phe (a) and L-Leu (b). Bars indicate standard/deviation for three measurements.

The V412L-PmaLAAD shows only a marginal increase of V_{\max} on the reference substrate (L-Phe) and on L-Leu in comparison with the wild-type enzyme. Unfortunately, the apparent K_m on L-Leu was 7-fold increased, resulting into a lower catalytic efficiency on this substrate in comparison to the wild-type PmaLAAD as also observed for L-Phe. For this reason, the V412L-PmaLAAD is not useful biocatalyst.

3.3 Alternative strategies to improve PmaLAAD substrate specificity

Introduction

L-Amino acid deaminases (LAADs, EC 1.4.99.B3) are membrane-bound flavoenzymes that use flavin adenine dinucleotide (FAD) as cofactor to catalyze the stereospecific oxidative deamination of L-amino acids to produce the corresponding α -keto acids and ammonia. LAADs do not produce hydrogen peroxide during catalysis. Indeed, these membrane-bound LAADs employ a noncanonical reoxidation mechanism: the reduced cofactor is reoxidized by transfer of an electron coupled to a suitable electron acceptor in the bacterial membrane. Electrons are eventually transferred through an electron transport chain to molecular oxygen with the formation of a water molecule^{2,3}. Since membrane-bound LAADs do not produce H₂O₂, these enzymes can be successfully overexpressed in prokaryotic hosts and can be used in mild reaction conditions (without the addition of catalase) during industrial biocatalysis^{4,5}. Consequently, a series of LAAD-based biocatalytic processes were developed for the eco-friendly and efficient production of pure D-amino acids and α -keto acids⁶⁻⁹.

Previous attempt to modify (widen) the substrate specificity of PmaLAAD by site-saturation mutagenesis, allowed the identification of improved variants of the enzyme, more active on the synthetic bulky substrate L-1-naphthylalanine¹. Unfortunately, no variants were identified possessing a significantly enhanced activity toward other natural or synthetic L-amino acids of biotechnological interest (e.g., L-Ser or substituted L-phenylglycines). This suggests that a protein engineering approach consisting in the substitution of only one or two residues of the active site of PmaLAAD would not result into a significantly altered substrate specificity. For this reason, we investigated the simultaneous introduction of several substitutions in the substrate binding pocket of PmaLAAD. In order to avoid obtaining “huge” libraries of variants, which would require a time-consuming screening procedure to identify improved variants, the identification

of the residues to be mutated was based on computational methods and on the rational analysis of the structure/function relationships in PmaLAAD.

3.3.1 Conversion of the type-I PmaLAAD into a type-II L-amino acid deaminase

Only bacteria belonging to the genus *Proteus* express LAADs. Each *Proteus* species expresses two different types of LAADs, which share a significant sequence similarity (~57%) but differ in substrate preference. The type-I LAADs (such as PmaLAAD or PmirLAAD from *P. myxofaciens* or *P. mirabilis*, respectively) are preferentially active on large aliphatic and aromatic amino acids. On the other hand, the type-II LAADs (such as pvLAAD or Pm1LAAD from *P. vulgaris* or *P. mirabilis*, respectively) show significant activity on charged and basic L-amino acids such as histidine and arginine.

Recently, the tridimensional structures of type-I PmaLAAD ² and of type-II pvLAAD ³ were solved. These two proteins show a very similar tertiary structure (the RMSD was 0.72 Å when the main chain atoms are superimposed), but possess a significantly different (and partially complementary) substrate scope (Tab. 1).

We used the knowledge on the active site residues of PvLAAD as a reference to alter the substrate specificity of PmaLAAD and to increase its activity toward polar (or even charged) substrates. After a structural comparison, we identified the residues differing between the two enzymes and replaced each of these residues of PmaLAAD with the corresponding residue of PvLAAD.

Table 1. The substrate specificity of PmaLAAD ², ΔN- pvLAAD ³ and pvLAAD ¹⁰.

Amino acid	Specific activity (%)		
	PmaLAAD ²	ΔN-PvLAAD ³	PvLAAD ¹⁰
Ala	0.6	80.0	3.5
Arg	8.0	38.0	27.3
Asn	0.7	87.0	43.6
Asp	0.1	38.0	55.4
Cys	43.0	7	0
Gln	0.6	0	1.1
Glu	0.1	0	1.1
Gly	0.1	0	0
His	10.0	60.0	79.9
Ile	26.0	50.0	0
Leu	99.0	92.0	105.0
Lys	3.0	36.0	3.5
Met	86.0	100.0	100.0
Phe	100	80.0	37.4
Pro	1.0	0	0.7
Ser	0.0	39.0	0
Thr	0.0	0	1.1
Trp	61.0	48.0	41.6
Tyr	14.0	77.0	92.8
Val	3.5	80.0	0

Materials and Methods

Computational analysis

Computational comparison between the active binding sites of PmaLAAD (PDB code 5FJM) ² and pvLAAD (PDB code 5HXW) ³ was performed using the software PyMol.

Multi site-directed mutagenesis

Multi-point mutations were generated by QuickChange multisite-directed mutagenesis kit (Agilent Technologies, Santa Clara, CA, USA). The genes coding for the V438G PmaLAAD variant ¹ was used as template. The primers employed for PCR reactions are reported in Table S1. The template DNA was

eliminated by enzymatic digestion with the *DpnI* restriction enzyme, specific for methylated DNA. The amplification mixture was used to transform *E. coli* NEB 10- β cells (the host for cloning). Introduction of the desired mutations was confirmed by automatic DNA sequencing. The plasmid DNA, which contains all desired substitutions, was then extracted from *E. coli* NEB 10- β cells and used to transform *E. coli* BL21(DE3) cells (the host for protein expression).

Expression and purification

Recombinant S99G/L279Q/A314S/F318I/V412M/V438G PmaLAAD variant (named, 6M-PmaLAAD) was produced as reported in *Motta et al*, 2016². The recombinant enzyme was purified in a single step by affinity chromatography². Cell pellets recovered from 1 L fermentation broth were resuspended in lysis buffer (50 mM potassium phosphate buffer pH 7.5, 5 mM MgCl₂, 1 mM PMSF, 1 mM pepstatine, and 10 μ g/mL DNase) and sonicated (6 cycles of 30 s each, with a 30 s interval on ice). The insoluble fraction of the lysate was removed by centrifugation at 39000 x g for 45 min at 4 °C. The crude extract was loaded onto a HiTrap chelating affinity column (5 mL GE Healthcare pre-loaded with 1 mL of 100 mM NiCl₂) equilibrated in binding buffer (50 mM sodium phosphate, pH 7.5, 1 M NaCl, 20 mM imidazole). The bound protein was eluted with a step gradient of the elution buffer (50 mM sodium phosphate, pH 7.5, 500 mM imidazole). PmaLAAD variants were eluted at 200 mM imidazole. The fractions containing the enzyme of interest were dialyzed overnight against 50 mM sodium phosphate, pH 7.5, 10% glycerol, using a 30 kDa-cutoff dialysis tube. PmaLAAD concentration was calculated based on the extinction coefficient at 456 nm of 14,168 M⁻¹ cm⁻¹ (determined for the wild-type enzyme).

Purification of *E. coli* membranes

The crude extract obtained by lysis of *E. coli* BL21(DE3):pET11a cells were subjected to ultracentrifugation at 150000 \times g for 2 hours to separate the cytoplasmic fraction (supernatant) from the membrane fraction (pellet). The

pellet was resuspended in 50 mM potassium phosphate buffer pH 7.5, 10% glycerol. This fraction was stored at -80 °C and used for LAAD activity assay.

Determination of the substrate specificity

Exogenous *E. coli* membranes were added to PmaLAAD variant (0.3 mg of membranes per µg of purified enzyme) and the enzyme was incubated for 30 min at room temperature before performing the screening of the activity on different substrates. PmaLAAD activity was assayed using 10 µg of enzyme mixture in presence of different L-amino acids (i.e., 50 mM L-Phe, 50 mM L-Met, 50 mM L-His, 50 mM L-Leu, Met, 50 mM L-Trp, 50 mM L-Asp, 50 mM L-Lys, 50 mM L-Ala, 50 mM L-Val, 50 mM L-Ser and 50 mM L-penicillamine) in 50 mM potassium phosphate buffer, pH 7.5 (final volume 250 µL). The substrate specificity of the 6M-PmaLAAD variant was investigated by means of a rapid colorimetric assay ¹. After incubation at 25 °C for 30', the production of the α-keto acid was measured by the quantification of the complex by the α-keto acid and the 2,4-dinitrophenylhydrazine (DNP) in basic environment. The absorbance at 450 nm was recorded by a microtiter plate reader (Infinite 200, Tecan, Mannedorf, Switzerland) and compared with wild-type PmaLAAD (positive controls).

Results

Comparison PmaLAAD vs. pvLAAD active site

The 3D structure of type-I PmaLAAD in complex with the inhibitor anthranilate (PDB code 5FJN) ² was superimposed to the 3D structure of type-II PvLAAD in complex with the detergent cetyl-trimethyl-ammonium (PDB code 5HXW) ² (Fig. 2). Eleven residues belonging to first shell have been identified (at < 6 Å from the ligand). From the superimposition, it is apparent that six of these residues are different between the two enzymes, namely: S99G, L279Q, A314S, F318I, V412M, V438G (where the first letter represents the residue of PmaLAAD while the second letter is the one at the active site of PvLAAD) (Fig. 1).

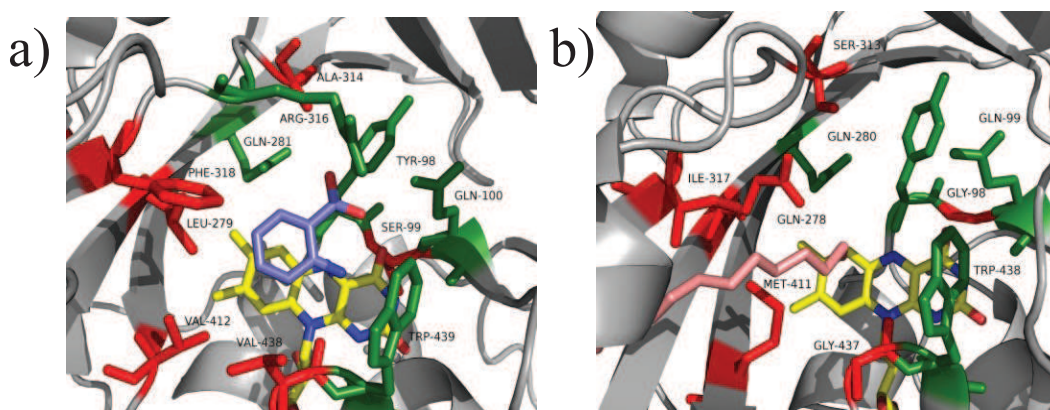


Figure 1. Comparison between the active site of (a) PmaLAAD in complex with the inhibitor anthranilate (blue) (PDB code 5FJN, left) and (b) pvLAAD in complex with the detergent cetyl-trimethyl-ammonium (pink) (PDB code 5HXW, right). Residues of PmaLAAD replaced with the residues of PvLAAD are represented in red.

Production of the S99G/L279Q/A314S/F318I/V412M/V438G-PmaLAAD variant (6M-PmaLAAD)

The residues identified by the computational analysis were simultaneously mutated using the oligonucleotides listed in Table S1 and the Quick Change multisite-directed mutagenesis kit to produce the 6M-PmaLAAD variant. The gene coding for the V438G-PmaLAAD (which was identified from site-saturation mutagenesis at position 438, see Melis et al., 2018¹) was used as a template in order to reduce the number of mutations that had to be simultaneously introduced. Insertion of the desired substitutions in 6M-PmaLAAD was confirmed by DNA sequencing. The variant was expressed in *E. coli* BL21(DE3) cells and purified by affinity chromatography². Recombinant 6M-PmaLAAD migrates as a single band at ~ 51 kDa with a degree of purity > 80% as estimated by SDS-PAGE (Fig. 2). The volumetric yield of pure 6M-PmaLAAD was 1.6-fold lower than the wild-type: 6.3 mg of pure protein/L_{culture} (0.6 mg of pure protein/g_{cells}) in comparison to 9.9 mg of pure protein/L_{culture} (1.0 mg of pure protein/g_{cells}) for the wild-type. The absorption spectrum of the purified 6M-PmaLAAD variant is similar to the canonical one of FAD-containing flavoprotein oxidases with two peaks in the visible region (385 nm

and 456 nm) due to the presence of the oxidized FAD cofactor and a higher peak in the UV region (at 273 nm). The spectrum was similar to the one of the wild-type enzyme (Fig. 2b). This suggests that the 6 substitutions introduced in the PmaLAAD active site do not significantly alter the polarity of the FAD microenvironment.

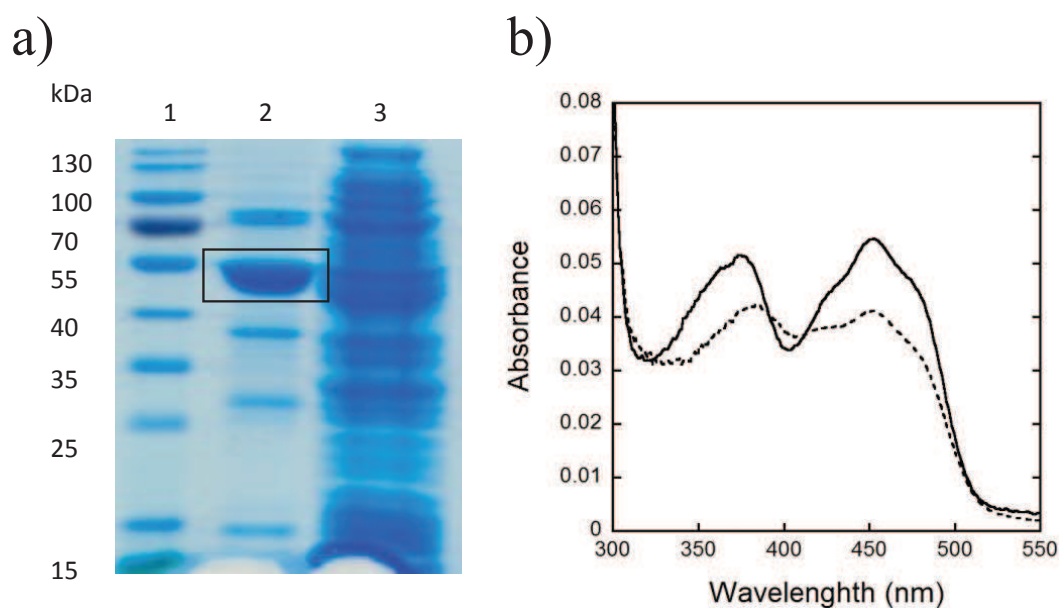


Figure 2. a) SDS-PAGE analysis of purified 6M-PmaLAAD. Lane 1: LMW markers (Prestained Protein Ladder, PageRuler™); lane 2: 5 µg of pure 6M-PmaLAAD variant and lane 3: 80 µg of 6M-PmaLAAD crude extract. b) Absorption spectrum of PmaLAAD (continuous line, R= 9.32) and 6M-PmaLAAD (dashed line, R= 10.7).

Substrate specificity of 6M-PmaLAAD variant

The substrate specificity scope of the 6M-PmaLAAD was determined using a microtiter plate and the colorimetric activity assay described in Materials and Methods. The overall enzymatic activity of the 6M-PmaLAAD variant is significantly decreased on all the tested substrates (Fig. 3a) although the degree of this change is different for different substrates. In the case of the best substrates of wild-type PmaLAAD, the 6M-PmaLAAD showed a decrease of ~70% for L-Phe and L-Trp and ~85% for L-Met. The 6M-PmaLAAD does not show a significant activity on small, polar or charged L-amino acids (e.g., L-His

and L-Ala) that were already poor substrates for the wild-type enzyme and on L-Leu.

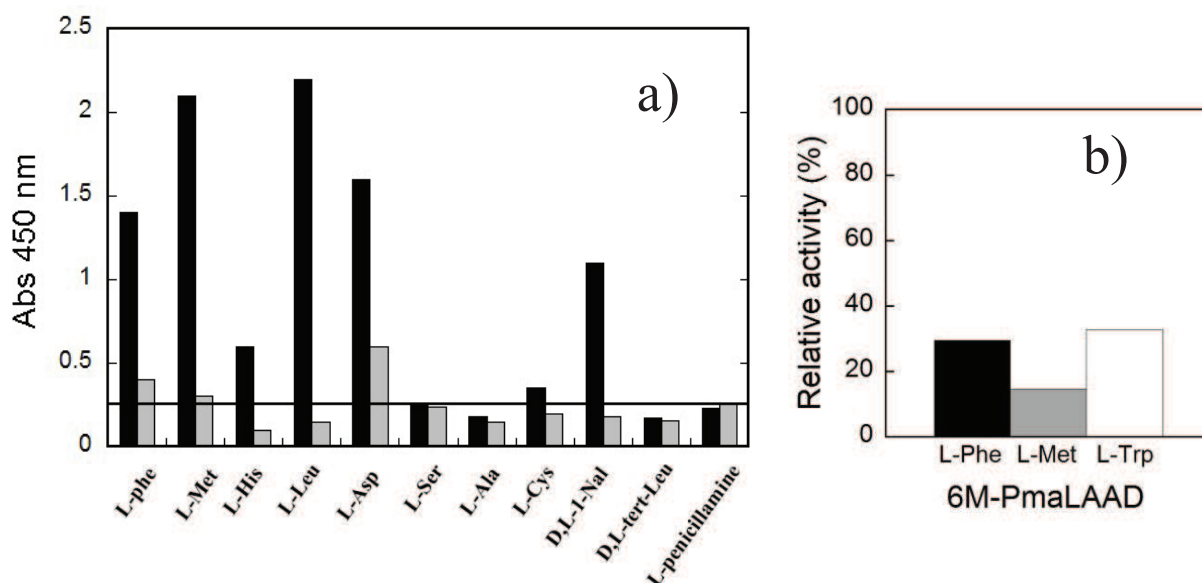


Figure 3. a) Absolute activity (as absorbance change at 450 nm) of the PmaLAAD (in black) and 6M-PmaLAAD variant (in grey). The horizontal line indicates the absorbance value (0.2) considered as a threshold for the activity detection. b) Relative activity of 6M-PmaLAAD on L-Phe (black), L-Met (gray) and L-Trp (white). The activity of PmaLAAD wild-type on the corresponding substrates is reported as 100%.

Conclusions

The substitution of 6 (out of 11) residues of the active site of PmaLAAD resulted into a variant which substrate scope did not resume the one of type-II LAAD, such as PvLAAD. Instead, the overall enzymatic activity is dramatically decreased (from ~ 65% in the case of L-Trp to almost 100% in the case of L-Leu). This suggests that the replacement of all the residues of the substrate specificity pocket of PmaLAAD with the ones of PvLAAD is not sufficient to switch the substrate specificity of the enzyme. It is plausible that, notwithstanding the overall high structural similarity between type-I and type-II enzymes, the different substrate scope is due to differences in the second shell residues of the active site and/or to a different flexibility/plasticity of specific regions of the substrate binding domain, which (indirectly) affect the substrate preference of the enzyme.

3.3.2 *PmaLAAD* ancestral active site

It is well accepted that, during the evolution enzymes changed from a more generalist form, with a wide substrate scope and a relative low affinity for the substrates and catalytic efficiency, to a more specialized form possessing higher catalytic efficiency on a small number of substrates (or even just one) ¹¹. Based on this observation, it has been proposed to change the substrate specificity of an enzyme by a directed evolution methods starting from the putative ancestral generalist form of the enzyme. In such a way, the *in vitro* evolution approach faithfully reproduces the natural evolution.

Ancestral proteins represent variants of present day enzymes whose combinations of substitutions have already been explored by nature and proven to be (at least partially) functional and stable.

These ancestral forms are no more experimentally accessible but their sequences can be inferred from phylogenetic trees. Concerning the substrate specificity, the attention can be focused on residues that are located within 6 Å of the substrate binding site. Variants obtained acting on these positions result in substitutions that are frequently seen in evolution and do not represent the entire hypothetical diversity. The ancestral reconstruction analysis has become a standard tool for protein engineering and is based on the use of evolutionary information preserved in the sequence of homologous proteins ^{12,13}.

Here, we engineered the *PmaLAAD* enzyme using this approach with the aim to improve its substrate specificity. Each first-shell residue of the substrate binding pocket of *PmaLAAD* was replaced with amino acid residues present in a putative ancestral sequence of *PmaLAAD*.

Materials and Methods

Ancestral reconstruction analysis

Multiple sequence alignment (MSA) of proteins homologous to *PmaLAAD* was built using the evolutionary conservation analysis tool ConSurf ¹⁴. Only proteins possessing an amino acid identity between 35% and 95% were considered. MSA of homologous sequences was used to generate a phylogenetic tree (NJ method)

and the most probable ancestral sequences for each node were predicted by the FastML server¹⁵.

Multi site-directed mutagenesis

Multi-point mutations were generated by QuickChange multi site-directed mutagenesis kit (Agilent Technologies, Santa Clara, CA, USA). The genes coding for the PmaLAAD was used as template. The primers employed for PCR reactions are reported in Table S1. The template DNA was eliminated by enzymatic digestion with the *DpnI* restriction enzyme, specific for methylated DNA. The amplification mixture was used to transform *E. coli* NEB 10-β cells. Introduction of the desired mutations was confirmed by automatic DNA sequencing. The plasmid DNA, which contains all desired substitutions, was extracted from *E. coli* NEB 10-β cells and used to transform *E. coli* BL21(DE3) cells (the host for protein expression); recombinant cells were used for the screening on different substrate as detailed below.

High-throughput screening for ancestral PmaLAAD variants

The substrate specificity of the clones that express ancestral PmaLAAD variants, expressing the L279S/F318A/V412I/V438G/W439H (namely, 5M), F318A/V412I/V438G/W439H (4M) and L279S/F318A/V412I (3M) substitutions were investigated by means of a rapid colorimetric assay detecting the produced α-keto acids using 2,4-dinitrophenylhydrazine (DNP) and by employing the epMotion 5075 automated liquid-handler system¹. *E. coli* cultures grown at saturation (1 mL in DeepWell plate, Eppendorf, Hamburg, Germany) were added of 0.1 mM IPTG, incubated at 28 °C for 4 h and stored at 4 °C overnight. The next day, 200 μL of each culture was centrifuged at 4000 × *g* for 5 min and the cell pellet was resuspended with 1 mL of 10 mM Tris-HCl, 1 mM EDTA, 100 mM NaCl, pH 8.0. Subsequently, 100 μL of resuspended cells were lysed by adding 900 μL of 40 μg/mL lysozyme solution (30 min, 37 °C). Then, 50 μL of the crude extract were transferred into a well of a 96-well plate. LAAD activity was assayed on the crude extract by adding 50 μL of substrate (50 mM L-Phe, 50

mM L-Leu, 50 mM L-Met, 50 mM L-Asp, 50 mM L-His, 50 mM L-Cys, 50 mM L-Ala, 50 mM L-Ser, 50 mM D,L-tert-Leu, 5 mM *p*-CH₃O-PheGly, 50 mM L-penicillamine and 1.2 mM D,L-1-Nal) in 50 mM potassium phosphate buffer, pH 7.5. After incubation at 25 °C for 2 h, production of the α -keto acid was measured by the colorimetric assay. The absorbance at 450 nm was recorded by a microtiter plate reader (Infinite 200, Tecan, Mannedorf, Switzerland) and compared with the values obtained for cultures expressing the wild-type PmaLAAD (positive controls) and untransformed *E. coli* cells (negative control).

Expression and purification

Recombinant PmaLAAD variants were produced as reported in *Motta et al*, 2016². The recombinant enzymes were purified in a single step by affinity chromatography² (see before).

Results

Design and production of ancestral PmaLAAD variants

The amino acid sequence of PmaLAAD (from the PDB entry 5FJN) was used as input for the evolutionary conservation analysis (ConSurf). To avoid not-significant hits, sequences with an amino acid identity lower than 35% were excluded from the multiple sequence alignment (MSA). In addition, to prevent any bias, redundant sequences exhibiting $\geq 95\%$ were clustered and only one representative sequence for each cluster was used for MSA. MSA of homologous sequences was used to generate a phylogenetic tree and the most probable ancestral sequence for the first node (i.e. the most “ancient” node of the phylogenetic tree which was in common with all the leaves of the tree) was predicted¹⁵. The predicted sequence of the node 1-ancestral protein was aligned to PmaLAAD in order to identify amino acid differences between the two proteins showing an overall 42% amino acid identity (Fig. 4a). As shown in Figure 4b (green residues), positions 279, 318, 438, and 439 show the most different residues between the node 1-ancestral sequence and PmaLAAD sequence: this suggests that residues in this region of the active site are the most

evolvable positions that allowed LAAD to modify its substrate specificity during natural evolution ¹³.

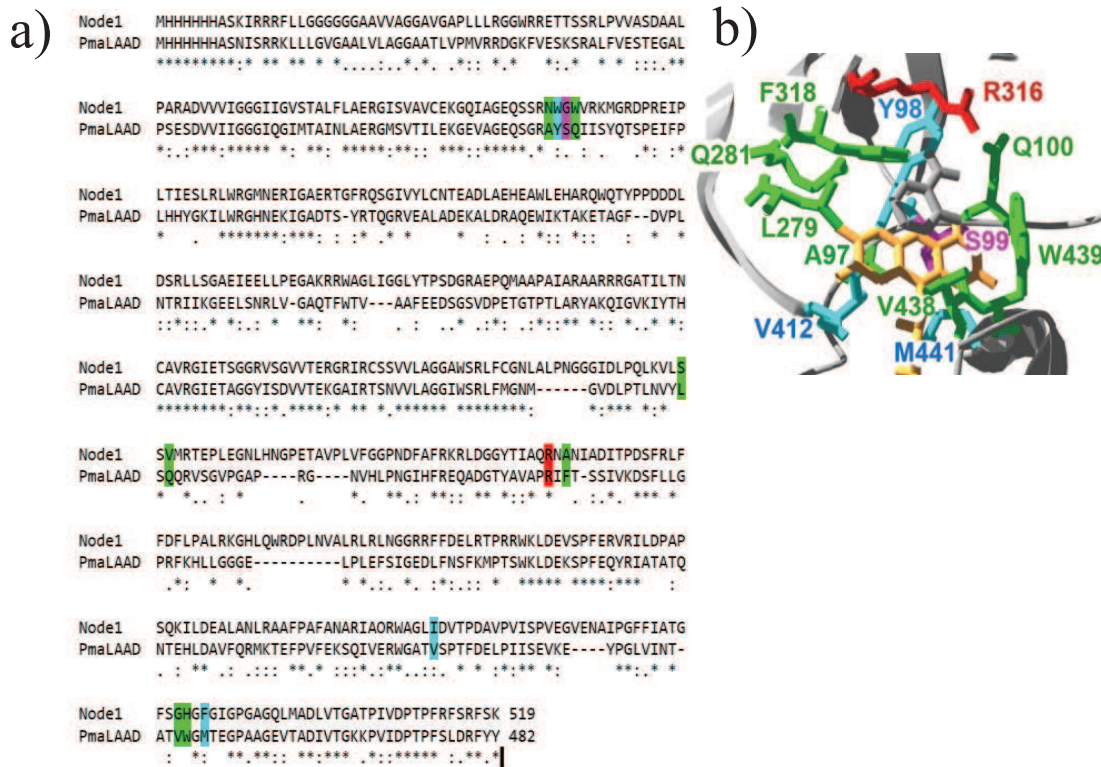


Figure 4. a) Amino acid alignment between PmaLAAD and the most probable ancestral sequence of node 1. b) Detail of the active site of PmaLAAD at distance < 6 Å. The amino acid residues are colored by their degree of conservation (see alignment): red, conserved; cyan, highly similar; purple, poorly similar; green, different.

Interestingly, the sole conserved residue between the active site of the node 1-ancestral LAAD and PmaLAAD is Arg316. Indeed, Arg316 forms a 2-point electrostatic interaction with the substrate carboxyl group thus representing a key residue for the binding of the substrate (Fig. 4b). In addition, this residue changes its orientation following substrate binding ¹.

On the basis of the phylogenetic analysis we decided to introduce the residues of the node 1-ancestral LAAD at positions L279, F318, V438, W439 and at position V412 (a residue substituted with a similar amino acid in node 1 protein, cyan in Fig. 4) of the first shell. Notably, variants at this latter position showed an increase activity toward L-1-Nal ⁹. Multi site-directed mutagenesis was

performed using the oligonucleotides listed in Table S1, and the cDNA coding for PmaLAAD-00N as a template. Three different variants were produced possessing a different number of mutations: the L279S/F318A/V412I/V438G/W439H-PmaLAAD (5M-PmaLAAD), F318A/V412I/V438G/W439H-PmaLAAD (4M-PmaLAAD) and L279S/F318A/V412I-PmaLAAD (3M-PmaLAAD).

Biochemical analysis of ancestral PmaLAAD variants

The activity of the three variants on different substrates was evaluated using a microtiter plate and the colorimetric activity assay described in Materials and Methods using 50 μ L of crude extracts¹. No variants showed a significant activity on the tested substrates. Interestingly, the loss of activity of the variants is proportional to the number of substitutions: the 5M- and 4M-PmaLAAD variants lost the enzymatic activity on all tested substrates, while the 3M-PmaLAAD variant maintains a residual activity on different substrates: L-Phe, L-Leu, L-His, L-Met and D,L-1-Nal (Fig. 5).

All variants were purified by affinity chromatography (IMAC). In all cases, the volumetric yield of the pure protein was significantly lower than the value obtained for the wild-type enzyme as observed by SDS-PAGE (data not shown). The absorbance spectrum of the purified 5M- and 4M-PmaLAAD variant is substantially different from the wild-type one suggesting that these variants are produced as apoproteins (data not shown). Only the 3M-PmaLAAD was obtained as holoprotein: the volumetric yield was \sim 7-fold (0.26 mg/L_{culture}) lower than the one of the wild type.

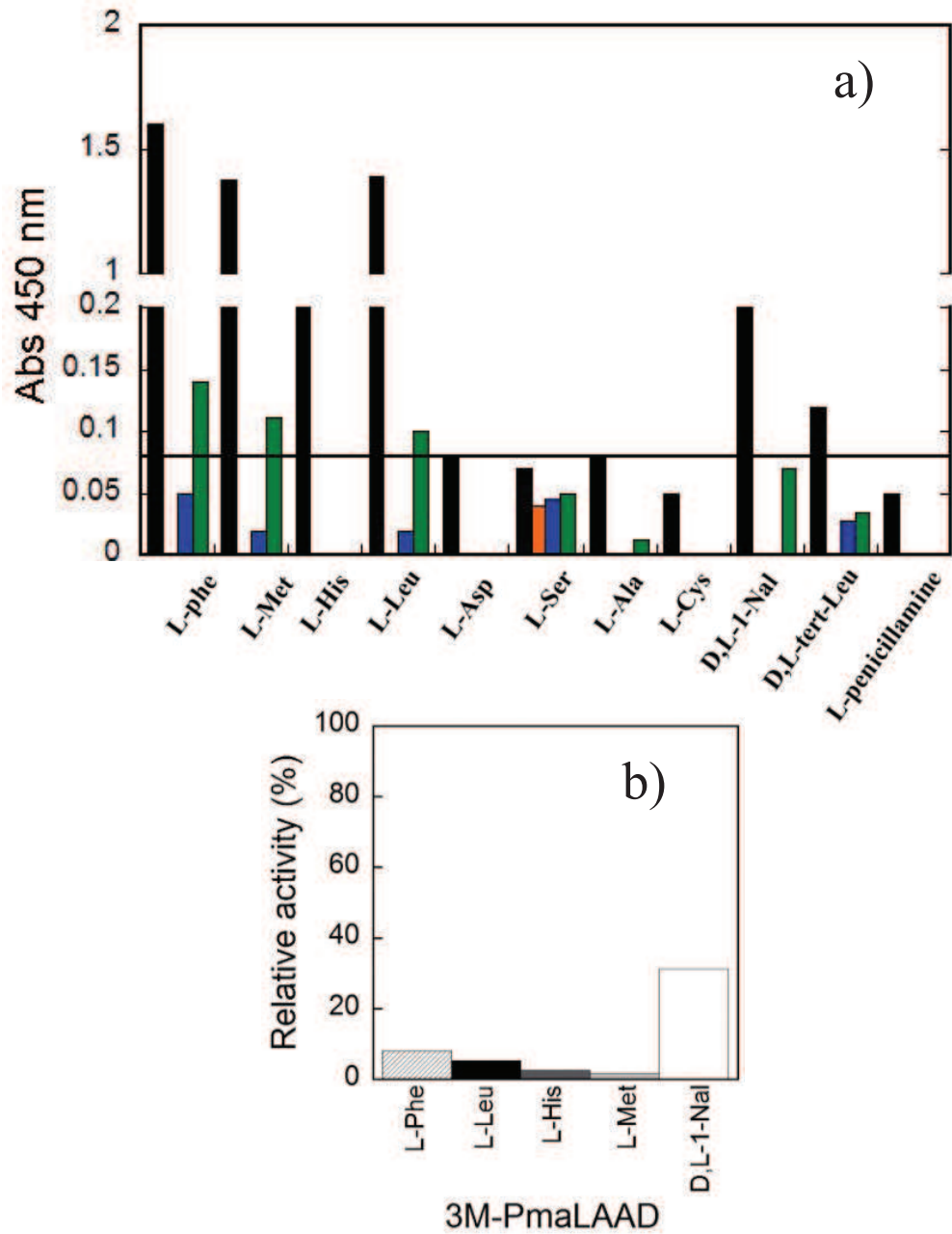


Figure 5. a) Activity (expressed as absorbance increase at 450 nm) of wild-type PmaLAAD (black), 5M-PmaLAAD (orange), 4M-PmaLAAD (blue) and 3M-PmaLAAD (green). The line indicates the absorbance value taken as a threshold. b) Relative activity of 3M-PmaLAAD variant. Enzymatic activity is shown as relative value: the activity of wild-type PmaLAAD on the corresponding substrate is taken as 100%. Activity was determine on 50 mM L-Phe (striped), L-Leu (black), L-His (gray), L-Met (light gray), 1.2 mM D,L-1-Nal (white).

Conclusions

The introduction of “ancestral” residues at selected positions of the active site of PmaLAAD generated variants with an impaired ability to bind the cofactor and, consequently, with only a marginal residual activity on several substrates. We can envisage two main reasons for these unexpected results; i) the choice of the most distant ancestral sequence (node 1 protein) as a reference, which lead to the introduction of the less conservative substitutions; ii) the introduction of several substitutions only in the first shell of the active site, which could have altered the protein structure impairing its stability. Concerning this latter point, it is conceivable that introduction of additional substitutions by an additional round of random mutagenesis could lead to the introduction of “compensatory” mutations that eventually could restore the enzyme activity. Unfortunately, at the moment, this strategy cannot be pursued because it requires a very high-throughput method of screening that is not yet available. The most desirable scenario is the production of a “full” node 1-ancestral protein (which carries all the 200 mutations (out of 482 residues, including the 6xHisTag and excluding the putative N-terminal transmembrane α -helix) could result into the production of a stable and active ancestral PmaLAAD.

3.3.3 Rational design of a PmaLAAD variant active on L-penicillamine

Semi-rational design, which combines directed evolution with rational design approaches to create small library of very high quality, have gained a great relevance^{16,17}. This approach is based on a detailed structural computational analysis, which can include the knowledge of the structure-function relationships of the protein, a sequence homology analysis and/or the use of predictive computational algorithms (e.g., molecular docking analysis, evolutionary conservation). These *in silico* approaches allow to focus the protein engineering efforts on regions of the target enzyme in which substitutions have the highest chance to result into production of the desired variants. In this way strategy the

library size and the subsequent screening efforts are reduced, allowing to efficiently sample the sequence space ¹².

Penicillamine (PenA) is a well-known metal chelating compound that has been successfully used for the treatment of Wilson disease since its introduction in 1956 ¹⁸. After more than 60 years of therapeutic use for the Wilson disorder, PenA is currently also used in the treatment of rheumatoid arthritis, cystinuria and heavy metal intoxication ¹⁹. This compound is a structural analog of cysteine: it differs from the amino acid by the presence of two methyl-groups on the β -carbon. PenA is a chiral compound which exists as D- and L-enantiomers; similarly to other chiral drugs, pharmacological effects of the two enantiomers differ considerably. D-PenA is the enantiomer which has the highest clinical effect, but the toxicity of the L- form restricts its therapeutic dosage ²⁰. For this reason, the resolution of PenA racemic mixture for pharmaceutical preparations is of biotechnological relevance ²¹. For this application, enantioselective biocatalysis should represent a competitive approach in comparison to chemical enantiomeric resolution methods.

Exploiting the knowledge of the 3D structure of PmaLAAD ², we designed a semi-rational design approach to produce PmaLAAD variants active on L-PenA. These variants will be exploited for the production of optically pure D-PenA by the enzymatic resolution.

Materials and Methods

Docking analysis

Molecular docking analysis was performed using the software Autodock Vina ²². PyMol was used for analysis of docking results.

Multi site-directed mutagenesis

Multi-point mutations were generated by QuickChange lightning multi site-directed mutagenesis kit (Agilent Technologies, Santa Clara, CA, USA). The gene coding for PmaLAAD-00N ² was used as template. The primers employed

for PCR reactions are reported in Table S1. The PCR products were used to transform NEB 10- β *E. coli* cells for the production of the variant library. The random pool of the recombinant plasmids was transferred to BL21(DE3) *E. coli* cells, which were subsequently screened for L-amino acid deaminase activity.

High-throughput screening for evolved PmaLAAD variants

The plasmid DNA pools containing the whole genetic variability generated by multi site-directed mutagenesis were transferred to the *E. coli* BL21(DE3) expression strain (Merck, Milano, Italy) to perform a screening for enzymatic activity. The variant libraries obtained from multi site-directed mutagenesis were screened on 25 mM L-Phe and 25 mM L-PenA in 50 mM potassium phosphate buffer, pH 7.5, by means of a rapid colorimetric assay detecting the produced α -keto acids using 2,4-dinitrophenylhydrazine (DNP) and by employing the epMotion 5075 automated liquid-handler system (Eppendorf, Hamburg, Germany) (for details see the high-throughput screening in *Melis et al., 2018*¹).

Results

Docking analysis: the PmaLAAD:L-penicillamine complex

The residues of PmaLAAD potentially involved in L-penicillamine binding were identified by molecular docking analysis. The crystallographic structure of PmaLAAD-01N without the putative transmembrane α -helix and in complex with anthranilate (PDB code 5FJN)² was used as the receptor to predict the mode of binding of the substrate L-PenA to the enzyme (Fig. 6 and Tab. S2). The analysis of the predicted PmaLAAD:L-PenA complex showed that an enhanced affinity for L-PenA could be obtained by reducing the size of the substrate specificity pocket and by substituting the hydrophobic residues of wild-type PmaLAAD with residues able to form (weak) sulfur H-bonds with the ligand SH group²¹. Three residues (Phe318, Val412 and Val438) were identified in close contact with the substrate side chain and potentially able to form an H-bond if replaced by polar residues (Fig. 6b).

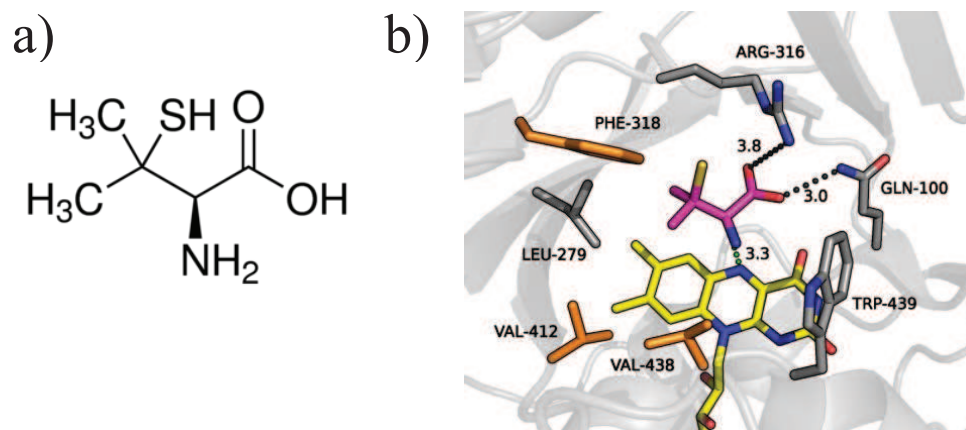


Figure 6. Binding of L-penicillamine to PmaLAAD. a) Chemical structure of L-penicillamine. b) Detail of the active site of PmaLAAD in complex with the ligand L-PenA (purple) as predicted by molecular docking simulations. Residues in close contact with the substrate side chain and subjected to site-saturation mutagenesis are shown in orange.

Production of PmaLAAD variant and screening on L-PenA

Each of the three residues Phe318, Val412 and Val438 was replaced with three different polar and/or large residues: in particular, we introduced Glu/Tyr/Trp at position 318, Asn/Leu/Gln at position 412 and Asn/Tyr/Gln at position 438.

In order to enhance the chance to obtain a variant possessing the desired property, each substitution was randomly and simultaneously inserted into these position using the QuickChange lightning multi site-directed mutagenesis kit and a suitable pool of mutagenic primers (Tab. S1) (see Material and Methods). This strategy allowed the generation of a small library containing 27 different triple variants (plus 37 double and single variants). The analysis of the gene sequences of random clones confirmed the genetic diversity in the produced library (Tab. S3). In order to perform a functional screening for enzymatic activity, the amplification mixture was used to transform *E. coli* BL21(DE3) cells obtaining a variant library of approximately 4000 colonies, a size sufficient for a suitable genetic diversity. PmaLAAD variants were screened for the activity on 25 mM L-Phe (the reference substrate) and L-PenA (see Materials and Methods) on a

microtiter plate. A colorimetric assay for the detection of produced α -keto acids using 2,4-dinitrophenylhydrazine reagent was employed. 190 clones were screened, a number that gives a probability > 95% to analyze each potential variant. Only 36% of PmaLAAD variants retained a residual activity on the reference substrate L-Phe and no variant showed a significant activity on L-penicillamine (Data not shown).

Conclusions

The simultaneous substitution of three key residues at the substrate specificity pocket of PmaLAAD (Phe318, Val412 and Val438) with a small subset of residues resulted into a high fraction of inactive variants (~ 64%). We must remark that, although the fraction of inactive clones is very high, mutagenesis at other positions of the active site showed even high figures; e.g., site-saturation mutagenesis at positions 439 or S99/Q100 resulted into ~ 80% and ~ 85% of inactive clones, respectively ¹. Unfortunately, none of the potential combinations of the substituted residues allowed to obtain a variant active on L-PenA. This could depend on the fact that the active site of PmaLAAD (even the variants) is not suited to efficiently bind a “small” substrate. In addition, the potential H-bonds formed by the sulfur of L-PenA and the active site residue could be too weak to provide a significant binding-energy contribution to the binding of L-PenA ²³.

It is also possible that, from a mechanistic point of view, the substrate L-penicillamine can not be oxidized by PmaLAAD because of the lack of a β C-H bond and the impossibility to form a double bond during the first step of catalysis (see Discussion section of this thesis for details).

Supplementary Materials:

Table S1. Primers used for site-directed mutagenesis

Position	Primers for PmaLAAD pvLAAD-active-site like
S99	Forward: 5'-GAGCAATCAGGCCGCGCATACGGCCAAATCATTAGCTACC-3'
L279	Forward: 5'-CCAACCTTGAATGTTTACCAGTCACAACAACGTGTATC-3'
A314/F318	Forward: 5'-CGGCACTTATGCTGTAAAGCCCACGTATCATCACAAGCTCCATTG-3'
V412	Forward: 5'-GAACGTTGGGGTGCAGTTATGAGTCCAACATTTGATG-3'
V438	Forward: 5'-CAATACAGCGACAGGGTGGGGAATGACAGAAGGTCC-3'
Position	Primers for Ancestral PmaLAAD
L279	Forward: 5'-CCAACCTTGAATGTTTACAGTTCACAACAACGTGTATC-3'
F318	Forward: 5'-CTTATGCTGTAGCCCCACGTATCGCTACAAGCTCCATTG-3'
V412	Forward: 5'-GAACGTTGGGGTGCAGTTATTAGTCCAACATTTGATG-3'
V438/W439	Forward: 5'-CAATACAGCGACAGGGTCATGGAATGACAGAAGGTCC-3'
Position	Primers for Multi-Site Directed Mutagenesis
F318	Forward F318Q: 5'-CTTATGCTGTAGCCCCACGTATCCAGACAAGCTCCATTG-3'
	Forward F318Y: 5'-CTTATGCTGTAGCCCCACGTATCTACACAAGCTCCATTG-3'
	Forward F318W: 5'-CTTATGCTGTAGCCCCACGTATCTGGACAAGCTCCATTG-3'
V412	Forward V412L: 5'-GAACGTTGGGGTGCAGTTCTAAGTCCAACATTTGATG-3'
	Forward V412N: 5'-GAACGTTGGGGTGCAGTTAACAGTCCAACATTTGATG-3'
	Forward V412Q: 5'-GAACGTTGGGGTGCAGTTCAAAGTCCAACATTTGATG-3'
V438	Forward V438Q: 5'-CAATACAGCGACACAGTGGGGAATGACAGAAGGTCC-3'
	Forward V438N: 5'-CAATACAGCGACAAACTGGGGAATGACAGAAGGTCC-3'
	Forward V438Y: 5'-CAATACAGCGACATATTGGGGAATGACAGAAGGTCC-3'

Table S2. Docking energies of L-penicillamine to PmaLAAD.

mode	affinity (kcal/mol)	dist from best mode	
		rmsd l.b.	rmsd u.b.
1	-4.9	0.000	0.000
2	-4.7	1.093	1.322
3	-4.6	1.722	2.269
4	-4.5	2.096	2.383
5	-4.5	2.101	2.556
6	-4.5	1.849	2.331
7	-4.5	2.699	3.144
8	-4.4	1.681	1.856
9	-4.4	1.897	1.986

Table S3. Analysis of the genetic diversity of PmaLAAD libraries for the generation of variants active on L-penicillamine (generated by multi site-directed mutagenesis).

Position	Original codon	n° of sequence clones	Introduced mutation	Encoded residue	Number of mutations	Fraction of variants (%)
F318/V412 /V438	TTC/GTA/GTG	9	TGG/CAA/TAT	Trp/Gln/Tyr	3	100
			CAG/GTA/AAC	Gln/Val/Asn	2	
			CAG/CAA/CAG	Gln/Gln/Gln	3	
			TGG/CTA/GTG	Trp/Leu/Val	2	
			TGG/GTA/GTG	Trp/Val/Val	1	
			CAG/GTA/GTG	Gln/Val/Val	1	
			TGG/CAA/GTG	Trp/Asn/Gln	3	
			TGG/CAA/GTG	Tyr/Gln/Val	2	
			CAG/CTA/GTG	Gln/Leu/Val	2	

3.4.4 References

1. Melis, R., Rosini, E., Pirillo, V. Pollegioni, L., & Molla, G (2018). *In vitro* evolution of an L-amino acid deaminase active on L-1-naphthylalanine. Submitted.
2. Motta, P., Molla, G., Pollegioni, L., & Nardini, M. (2016). Structure-function relationships in L-amino acid deaminase, a flavoprotein belonging to a novel class of biotechnologically relevant enzymes. *Journal of Biological Chemistry*, 291(20), 10457-10475.
3. Ju, Y., Tong, S., Gao, Y., Zhao, W., Liu, Q., Gu, Q., & Zhou, H. (2016). Crystal structure of a membrane-bound L-amino acid deaminase from *Proteus vulgaris*. *Journal of Structural Biology*, 195(3), 306-315.
4. Molla, G., Melis, R., & Pollegioni, L. (2017). Breaking the mirror: L-Amino acid deaminase, a novel stereoselective biocatalyst. *Biotechnology Advances*, 35(6), 657-668.
5. Song, Y., Li, J., Shin, H. D., Liu, L., Du, G., & Chen, J. (2016). Biotechnological production of α -keto acids: current status and perspectives. *Bioresource Technology*, 219, 716-724.
6. Rosini, E., Melis, R., Molla, G., Tessaro, D., & Pollegioni, L. (2017). Deracemization and stereoinversion of α -amino acids by L-amino acid deaminase. *Advanced Synthesis & Catalysis*, 359(21), 3773-3781.
7. Hossain, G. S., Li, J., Shin, H. D., Liu, L., Wang, M., Du, G., & Chen, J. (2014). Improved production of α -ketoglutaric acid (α -KG) by a *Bacillus subtilis* whole-cell biocatalyst via engineering of L-amino acid deaminase and deletion of the α -KG utilization pathway. *Journal of Biotechnology*, 187, 71-77.
8. Liu, L., Hossain, G. S., Shin, H. D., Li, J., Du, G., & Chen, J. (2013). One-step production of α -ketoglutaric acid from glutamic acid with an engineered L-amino acid deaminase from *Proteus mirabilis*. *Journal of Biotechnology*, 164(1), 97-104.
9. Hou, Y., Hossain, G. S., Li, J., Shin, H. D., Liu, L., Du, G., & Chen, J. (2016). Two-step production of phenylpyruvic acid from L-phenylalanine by growing and resting cells of engineered *Escherichia coli*: process optimization and kinetics modeling. *PloS one*, 11(11), e0166457.
10. Takahashi, E., Ito, K., & Yoshimoto, T. (1999). Cloning of L-amino acid deaminase gene from *Proteus vulgaris*. *Bioscience, Biotechnology, and Biochemistry*, 63(12), 2244-2247.
11. Khersonsky, O., Roodveldt, C., & Tawfik, D. S. (2006). Enzyme promiscuity: evolutionary and mechanistic aspects. *Current opinion in chemical biology*, 10(5), 498-508.
12. Porebski, B. T., & Buckle, A. M. (2016). Consensus protein design. *Protein Engineering, Design and Selection*, 29(7), 245-251.
13. Alcolombri, U., Elias, M., & Tawfik, D. S. (2011). Directed evolution of sulfotransferases and paraoxonases by ancestral libraries. *Journal of Molecular Biology*, 411(4), 837-853.
14. Landau, M., Mayrose, I., Rosenberg, Y., Glaser, F., Martz, E., Pupko, T., & Ben-Tal, N. (2005). ConSurf 2005: the projection of evolutionary conservation scores of residues on protein structures. *Nucleic Acids Research*, 33(Suppl. 2), W299-W302.

15. Pupko, T., Pe, I., Shamir, R., & Graur, D. (2000). A fast algorithm for joint reconstruction of ancestral amino acid sequences. *Molecular Biology and Evolution*, 17(6), 890-896.
16. Wijma, H. J., Floor, R. J., & Janssen, D. B. (2013). Structure-and sequence-analysis inspired engineering of proteins for enhanced thermostability. *Current Opinion in Structural Biology*, 23(4), 588-594.
17. Lutz, S. (2010). Beyond directed evolution semi-rational protein engineering and design. *Current Opinion in Biotechnology*, 21(6), 734-743.
18. Walshe, J. M. (1956). Penicillamine, a new oral therapy for Wilson's disease. *The American Journal of Medicine*, 21(4), 487-495.
19. Ishak, R., & Abbas, O. (2013). Penicillamine revisited: historic overview and review of the clinical uses and cutaneous adverse effects. *American Journal of Clinical Dermatology*, 14(3), 223-233.
20. Weigert, W. M., Offermanns, H., & Degussa, P. S. (1975). D-Penicillamine-Production and Properties. *Angewandte Chemie International Edition in English*, 14(5), 330-336.
21. Bhushan, R., & Kumar, R. (2010). Enantioresolution of D,L-penicillamine. *Biomedical Chromatography*, 24(1), 66-82.
22. Trott, O., & Olson, A. J. (2010). AutoDock Vina: improving the speed and accuracy of docking with a new scoring function, efficient optimization, and multithreading. *Journal of Computational Chemistry*, 31(2), 455-461.
23. Van Bergen, L. A., Alonso, M., Palló, A., Nilsson, L., De Proft, F., & Messens, J. (2016). Revisiting sulfur H-bonds in proteins: the example of peroxiredoxin AhpE. *Scientific Reports*, 6, 30369.

4. Discussion

The increasing demand of optically pure natural and synthetic amino acids from the fine chemicals, pharmaceutical and agrochemical industries spurs the development of novel, more efficient and environmentally-friendly processes for the asymmetric synthesis. In that respect, enzymes turned out to be competitive biocatalysts (in terms of yield and cost) in comparison to inorganic catalysts exploited in classical asymmetric synthesis. Enzymes possess several advantageous features such as a high (frequently absolute) chemo-, regio- and enantioselectivity, a high catalytic efficiency and require mild reaction conditions (i.e. pH close to neutrality, absence or low concentration of solvents and mild reaction temperature). Flavoprotein oxidases represent ideal enantioselective biocatalysts for the production of optically pure amino acids (for example by deracemization reactions) because of their absolute enantioselectivity and because they do not require the addition (and recycling) of expensive cofactors such as NAD⁺ during biocatalysis. In the past years, several protocols for the production of optically pure L-amino acids using the enantioselective yeast D-amino acid oxidase (or its engineered variants) as biocatalyst have been set-up^{1,2}. In principle, the specular reaction, catalyzed by an L-amino acid oxidase, could be used for the production of optically pure D-amino acids. These compounds have an high commercial importance because they are components of high added-value compounds such as antibiotics, pharmaceutical drugs, food additives, etc.³. D-amino acids are less frequent in Nature than L-amino acids and, consequently, their isolation from natural sources is more difficult. This results into an average higher economic value of these compounds compared with the corresponding L-enantiomers.

Unfortunately, the biocatalytic processes used for the production of pure L-amino acids cannot be directly exploited for the production of pure D-amino acids, since LAAO activities, suitable for large scale biotechnological applications, are not yet available⁴. In this respect, L-amino acid deaminases (LAADs) represent a convenient alternative to LAAOs since they can be efficiently expressed in *E. coli* and do not produce H₂O₂ during the catalysis⁵. As a matter of fact, several

LAADs from different sources were recently used as pure proteins or whole cell biocatalysts ⁶⁻⁹ (Fig. 1). The recent functional and structural characterization of the recombinant L-amino acid deaminase from *P. myxofaciens* (PmaLAAD) paved the way to its exploitation in enantioselective biocatalys ^{5,10,11}.

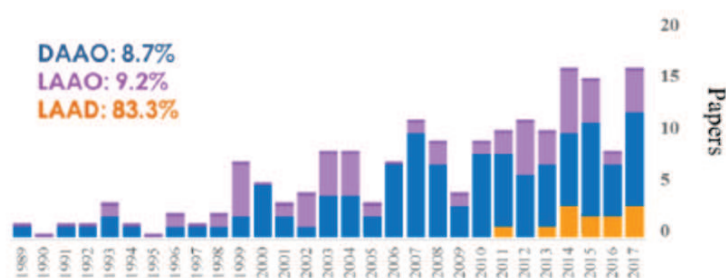


Figure 1. The scientific interest on biotechnological application of L-amino acid oxidases/deaminases and D-amino acid oxidases as biocatalysts. Bars represent the total number of papers published about each flavoprotein. Percentages represent the fraction of papers dealing with biotechnological applications of each enzyme.

The project reported in this PhD thesis can be divided into three main parts: 1) the development of new stereoselective biocatalytic processes at laboratory scale for the production of pure D-amino acids and α -keto acids exploiting PmaLAAD, 2) the improvement, by directed evolution of the activity of PmaLAAD on substrates of biotechnological interest such as L-Nal, and 3) the additional rational protein engineering studies to obtain PmaLAAD variants active on specific substrates of biotechnological interest (i.e., substituted phenylglycines or penicillamine).

Part 1

In order to overcome the major disadvantages of whole-cells biocatalysis, in all the bioreactions performed during the reported research activity, PmaLAAD was exploited as a pure enzyme (cell-free biocatalysis). This approach allowed to avoid a poor mass transfer due to the presence of the cell membrane barrier (this

is important especially for the biotransformation of synthetic substrates for which specific membrane transport systems are not present). In addition, also the potential depletion of the desired products or formation of side-products during biocatalysis due to the presence of aspecific additional enzymatic activities was avoided (for an example of such problems, see ¹²).

We demonstrated that PmaLAAD is a versatile biocatalyst that can be exploited to promote different kind of enantioselective biotransformations. For example, PmaLAAD can be used for the production of pure α -keto acids (e.g., phenylpyruvate or α -ketoisocaproate) from the corresponding L-amino acids or racemates. PmaLAAD can also be used for the production of optically pure D-amino acids through the deracemization of D,L-amino acid racemates or through the complete stereoinversion of an L-amino acid to the corresponding D-enantiomer (e.g., in the case of L-4-nitrophenylalanine, L-4-Npa), a compound that is used as starting point for the production of anti-fibrinolytic and plasmin inhibitors drugs ^{13,14}. The versatility of PmaLAAD is mainly due to its wide substrate specificity: this enzyme is active on several large hydrophobic (natural or synthetic) L-amino acids. A common feature of “generalist” enzymes is the ability to bind their substrates forming tight, yet aspecific, non-covalent interactions. From an energetic point of view, in this binding mode, van der Waals and hydrophobic interactions play a major role, while polar specific interactions (such as H-bonds or salt bridges) are limited to the binding of the “invariant” region of the substrate and, thus, do not participate in the definition of the substrate specificity of the enzyme. Accordingly, large hydrophobic residues line the substrate specificity pocket of PmaLAAD (Leu279, Arg316, Phe318, Val412, Val438, and Trp439) (Fig. 2).

A straightforward comparison between the performances in biocatalysis of PmaLAAD and other LAADs from different sources is difficult because of the different formulation of the biocatalysts (free enzymes vs. whole cells) and of the different reaction conditions (Tab. 1). Nonetheless, the PmaLAAD productivity on L-Phe (expressed as $(g_{\text{product}}/L)/(g_{\text{enzyme}}/L)/h$) is significantly higher than

Pm1LAAD¹⁵ on the same substrate (13.8 vs. 5.2, respectively) (Tab. 1). In addition, it must be pointed out that, in respect to LAAOs, PmaLAAD does not produce H₂O₂ during the reaction (which can be harmful for the enzyme and for the reaction products). For this reason, there is no need to add a ROS scavenger system (e.g., catalase) during biocatalysis, thus, facilitating the downstream-process, the product recovery and resulting into an additional reduction of the overall biotransformation costs.

The necessity of the addition of exogenous *E. coli* membranes to the enzyme preparation before biocatalysis should constitute an issue for the setup of bioreactions at laboratory scale (both, in terms of reproducibility and stability of the whole system). For this reason, we are investigating the replacement of bacterial membranes with artificial electron donors and detergents the at low concentration (P. Motta, personal communication).

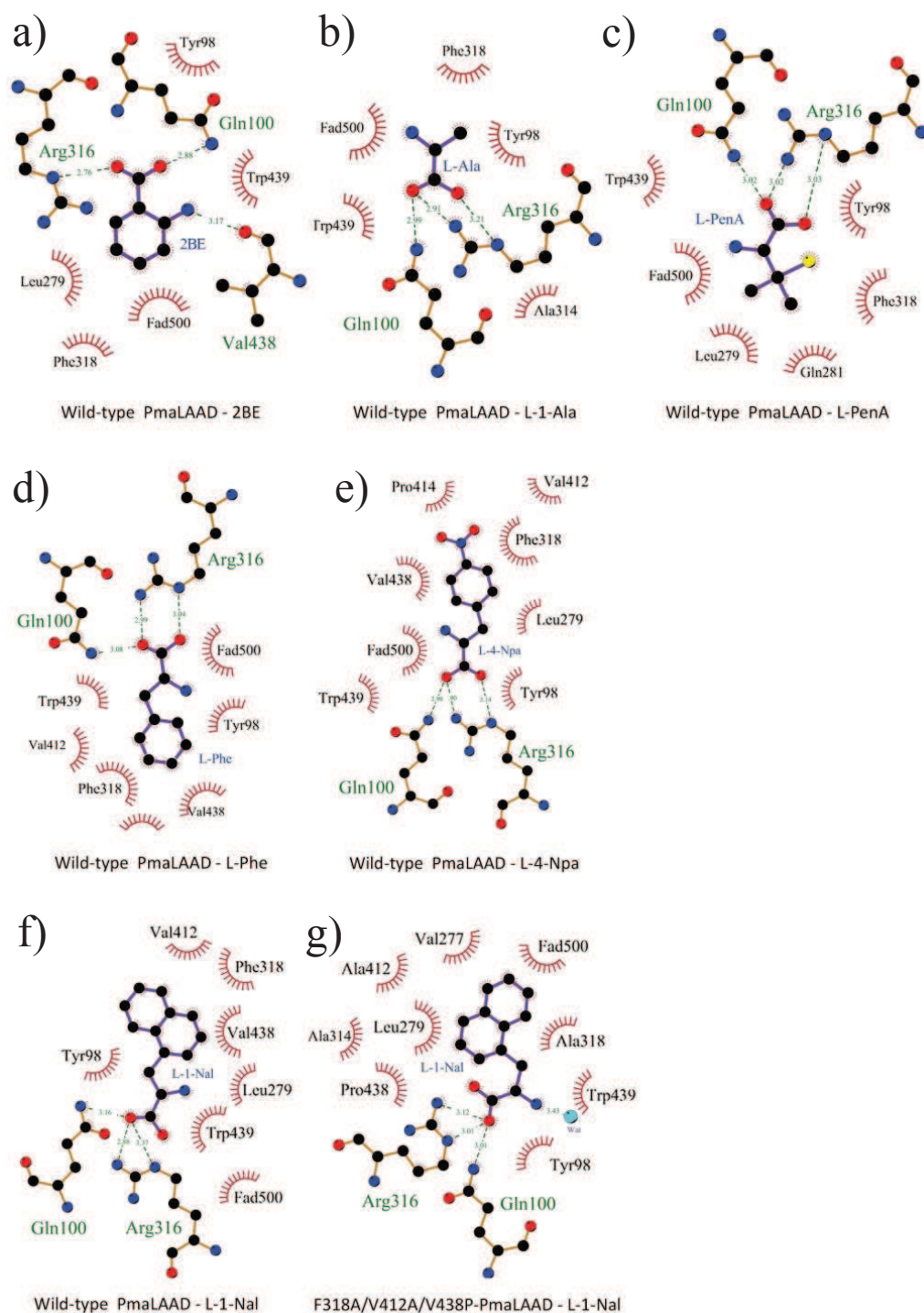


Figure 2. Schematic representation of the interactions between substrates (purple) and the active-site residues of wild-type (panels a-f) or F318A/V412A/V438P-PmaLAAD (panel g). Plots were generated using LigPlot⁺ ¹⁶ software and the following parameters: maximum H-bonds distance = 3.5 Å and maximum non-bonded contact distance = 4.3 Å. 2BE, anthranilate; L-PenA, L-penicillamine; L-Npa.

Table 1. Properties of L-amino acid deaminase biocatalysts.

Enzyme	Initial [L-substrate] (g L ⁻¹)	Substrate	Conversion yield (%)	Yield (g L ⁻¹)	Reaction time (h)	Biocatalyst formulation	Amount of biocatalyst (g biocatalyst L ⁻¹)	Productivity (g product/L)/(g enzyme/L/h)	Ref.
Type-I LAAD									
Pm1LAAD ^a	4	L-Phe	83	3.3	6	Whole-cell	1.2	0.46	15
Pm1LAAD ^a	3	L-Phe	87	2.6	2.5	Enzymatic biocatalyst	0.2	5.20	15
Pm1LAAD D165K/K263M/L336 M ^a	10 (fed-batch)	L-Phe	100	21.0	8	Whole-cell engineered	20	0.13	17
Pm1LAAD ^a	15	L-Glu	31	4.7	24	Whole-cell immobilized	20	0.01	18
Pm1LAAD-F110I/A255T/E349D/R228C/T249S/I352A ^a	15	L-Glu	83	12.2	24	Whole-cell engineered	20	0.03	12
pm11338g4-Pm1LAAD variant ^a	33	L-Glu	54	53.7	24	Whole-cell	20	0.11	19
Pm1LAAD pm11338g4-variant ^a	50 (fed-batch)	L-Glu	NA	89.1	30	Whole-cell	20	0.15	19
Pm1LAAD pm1ep3-variant ^a	50	D,L-Ala	29 [*]	14.6	36	Whole-cell engineered	20	0.02	20
PvLAAD ^b	70	L-Met	71	49.7	24	Whole-cell	20	0.10	21
PvLAAD K104R/A337S ^b	70	L-Met	91	63.6	24	Whole-cell	20	0.13	21

PvLAAD ^b	13.1	L-Leu	98	12.7	20	Whole-cell	0.8	0.79	22
Type-II LAAD b									
PmaLAAD ^c	11.3	L-Val	~ 20	2.0	12	Whole-cell	10	0.02	23
PmaLAAD N100H/F318T ^c	11.3	L-Val	~ 73	8.2	12	Whole-cell	10	0.07	23
PmaLAAD-00N ^c	4.1	L-Phe	>99	4.1	3	Enzymatic biocatalyst	0.1	13.8	24
PmaLAAD-00N ^c	2.6	L-4-Npa	>99	2.6	0.5	Enzymatic biocatalyst	0.1	52.6	24
PmaLAAD-00N ^c	0.26	D,L-1-Nal	>99 [*]	0.1	1.5	Enzymatic biocatalyst	0.05	1.73	25
F318A/V412A/V438 P-PmaLAAD ^c	0.26	D,L-1-Nal	>99 [*]	0.1	0.25	Enzymatic biocatalyst	0.05	10.4	25
DAAO									
RgDAAO M213G ^d	0.26	D,L-1-Nal	>99 [*]	0.1	2	Enzymatic biocatalyst	0.03	2.24	26

* Yield was calculated considering only the L-form of the substrate.

^{a)} *P. mirabilis*

^{b)} *P. vulgaris*

^{c)} *P. myxofaciens*

^{d)} *R. gracilis*

Part 2

Recently, the 3D structure of LAAD from *P. myxofaciens* (PmaLAAD) has been solved in the hosting laboratory ¹⁰. The detailed knowledge of the enzyme structure enabled the design of a semi-rational protein engineering strategy to improve the substrate scope and/or the catalytic efficiency of the enzyme.

It has been demonstrated that “small but smart” libraries of variants increase the chance to identify the desired improved biocatalysts ²⁷. For this reason, we exploited a comprehensive computational analysis to identify positions of the active site of PmaLAAD that were used as target for site-saturation mutagenesis (SSM, a semi-rational *in vitro* approach). All residues that were substituted belongs the first-shell of the active site.

Using this approach several variants of PmaLAAD possessing improved kinetic properties on L-1-Nal were identified. From an evolutionary point of view, *in vitro* evolution of PmaLAAD followed the “strong negative trade-off” trajectory in which the enzyme loses its efficiency on the reference substrate (L-Phe) before improving the activity on the novel substrate L-1-Nal. Actually, all variants show an increase of the catalytic efficiency on L-1-Nal that is accompanied by a significant decrease of the catalytic efficiency on the reference substrate L-Phe. These PmaLAAD variants show an increased specificity constant on L-1-Nal (i.e., the ratio between the catalytic efficiency of the enzyme on L-1-Nal and the reference substrate L-Phe). As a matter of fact, the best variant (F318A/V412A/V438P-PmaLAAD) possesses a > 100-fold increased specificity constant on L-1-Nal in comparison with the wild-type enzyme. The higher catalytic efficiency on L-1-Nal of this variant (10.41 vs. 1.49 U/mg/mM for the wild-type enzyme) is mainly due to a ~ 5-fold higher affinity for L-1-Nal (K_m is 0.17 mM). This is very important in the case of poorly soluble substrate, such as L-1-Nal, since the higher affinity allows to reach a relative higher enzymatic activity at low substrate concentration. In the case of the F318A/V412A/V438P-PmaLAAD variant, this results into an almost 3-fold higher reaction rate at 0.6

mM L-1-Nal (its maximal concentration a water) corresponding to $\sim 80\% V_{\max}$, than for the wild-type enzyme.

Interestingly, docking analysis showed that the increased affinity for this compound of the triple variant was not obtained by increasing specific interactions at the active site, but by ensuring the retention of a crystallographic water molecule at the active site of the F318A/V412A/V438P-PmaLAAD variant in complex with the bulky L-1-Nal complex allowing a better orientations of the substrate during the catalysis (Fig. 2g).

The improved variants were used to develop an efficient enzymatic biotransformation process to produce optically pure D-1-Nal or the corresponding α -keto acid naphthylpyruvate (which is not commercially available). In the latter case, the enzyme was used in combination with the M213G-D-amino acid oxidase (DAAO) variant ²⁶. Notably, the productivity of the F318A/V412A/V438P-PmaLAAD was not only higher than wild-type enzyme (10.4 vs. 1.7, respectively) but almost 8-fold higher than the M213G-DAAO variant ²⁶ on the D- enantiomer (Tab. 1).

The structural analysis of the models for the PmaLAAD variants allowed to explain their inability to bind and deaminate small and/or polar substrates (e.g., L-Ala, L-Ser, L-penicillamine, etc.). The volume of the active site of the wild-type enzyme is large enough to accommodate bulky substrates (such as L-Phe, L-Trp, L-1-Nal). Since the substrate specificity pocket is lined by large hydrophobic residues (L-Trp, L-Val, L-Phe), a “randomly-introduced” amino acid substitution is likely to further increase the active site volume, further weakening non-covalent hydrophobic interactions and thus dramatically decreasing the binding energy. In our opinion, this reduces the chance to generate a PmaLAAD variant active on a small substrate by introducing very few (1 to 3) substitutions at the active site by SSM.

Part 3

A more “random” *in vitro* evolution of PmaLAAD (e.g. the simultaneous substitution of several residues) requires the screening of a number of variants that is beyond the possibility for the screening protocol that was set up during this PhD project. For example, the screening of libraries of variants carrying three simultaneously substitution requires to check a number $> 3 \times 10^6$ of individual clones even when NNK primers are employed²⁸. This observation prompted us to explore novel (and more rational) protein engineering approaches based on a more thorough examination of the structure/function relationships in PmaLAAD. These approaches were: 1) the conversion of type-I PmaLAAD into a type-II LAAD (which shows a different substrate scope), 2) the production of an “ancestral” generalist LAAD, and 3) the “factorial” site-directed mutagenesis. Unfortunately, these approaches were not successful in obtaining improved PmaLAAD variants on different substrates. The reason of the scarce success of these latter attempts probably does not rely on the protein engineering strategy itself, but on the trade-off between the number of overall potential different clones, that could be generated and the screening efforts required. For example, both in the case of the conversion of type-I PmaLAAD into a type-II LAAD and in the production of the “ancestral” LAAD, only a small subset of the identified residues (the ones belonging to the first shell of the active site) were substituted. This opens to the possibility, in the next future, to exploit more deeply these approaches to obtain novel and further improved variants of PmaLAAD, even by combining the variants already produced by site-saturation mutagenesis.

All together, the different approaches of protein engineering used during this PhD project allow to propose that the “evolution” of PmaLAAD substrate specificity is a more ambitious task difficult than the evolution of the substrate specificity of other amino acid oxidases such as the D-amino acid oxidases^{1,29}. It is conceivable that, in PmaLAAD, several factors synergistically act to shape the substrate scope of the enzyme. In particular, small compounds (i.e., molecules with a volume smaller than $\sim 110 \text{ \AA}^3$) and/or compounds possessing a predicted

LogP \leq 3.0 (as estimated using Interactive LogP calculator www.molinspiration.com/services/logp.html) are not substrates of the enzyme: Accordingly, the predicted binding energy (estimated using Autodock Vina ³⁰) is inversely related to the ligand molecular volume (Fig. 3).

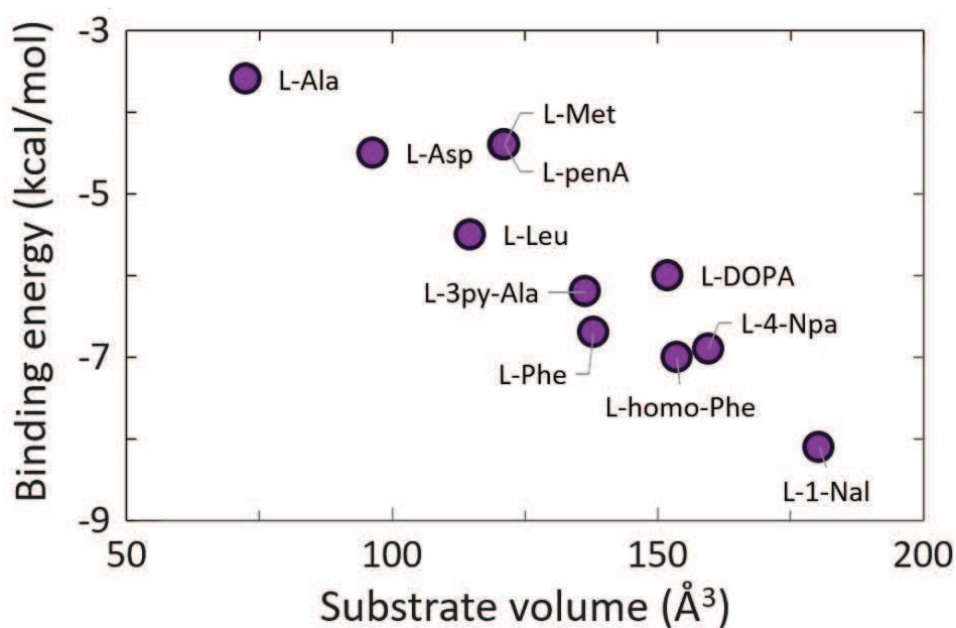


Figure 3. Estimated binding energy of different PmaLAAD substrates. Binding energy was predicted using Autodock Vina ³⁰. L-PenA: L-penicillamine; L-3py-Ala: L-pyridylalanine; L-4-Npa: L-4-nitrophenylalanine.

In addition, comparing of the activity of PmaLAAD on selected couples of substrates (i.e., L-Phe/L-phenylglycine, L-1-Nal/L-1-naphthylglycine) suggests that compounds unable to form an intermediate with a double bond between the C_α and C_β of the amino acid can not be oxidized by the enzyme. This could depend on the specific catalytic mechanism of the enzyme that has not yet investigated in details.

In conclusion, at present, PmaLAAD (both, the wild-type and the improved variants) represents the most reliable alternative to canonical LAOs for the

setup of enantioselective biocatalytic processes for the production of optically pure D-amino acids or α -keto acids.

4.1 References

1. Pollegioni, L., & Molla, G. (2011). New biotech applications from evolved D-amino acid oxidases. *Trends in Biotechnology*, 29(6), 276-283.
2. Pollegioni, L., Sacchi, S., Caldinelli, L., Boselli, A., Pilone, M. S., Piubelli, L., & Molla, G. (2007). Engineering the properties of D-amino acid oxidases by a rational and a directed evolution approach. *Current Protein and Peptide Science*, 8(6), 600-618.
3. Gao, X., Ma, Q., & Zhu, H. (2015). Distribution, industrial applications, and enzymatic synthesis of D-amino acids. *Applied Microbiology and Biotechnology*, 99(8), 3341-3349.
4. Pollegioni, L., Motta, P., & Molla, G. (2013). L-Amino acid oxidase as biocatalyst: a dream too far?. *Applied Microbiology and Biotechnology*, 97(21), 9323-9341.
5. Molla, G., Melis, R., & Pollegioni, L. (2017). Breaking the mirror: L-Amino acid deaminase, a novel stereoselective biocatalyst. *Biotechnology Advances*, 35(6), 657-668.
6. Alexandre, F. R., Pantaleone, D. P., Taylor, P. P., Fotheringham, I. G., Ager, D. J., & Turner, N. J. (2002). Amine-boranes: effective reducing agents for the deracemisation of D,L-amino acids using L-amino acid oxidase from *Proteus myxofaciens*. *Tetrahedron Letters*, 43(4), 707-710.
7. Hou, Y., Hossain, G. S., Li, J., Shin, H. D., Liu, L., Du, G., & Chen, J. (2016). Two-step production of phenylpyruvic acid from L-phenylalanine by growing and resting cells of engineered *Escherichia coli*: process optimization and kinetics modeling. *PloS one*, 11(11), e0166457.
8. Parmeggiani, F., Lovelock, S. L., Weise, N. J., Ahmed, S. T., & Turner, N. J. (2015). Synthesis of D-and L-phenylalanine derivatives by phenylalanine ammonia lyases: a multienzymatic cascade process. *Angewandte Chemie International Edition*, 54(15), 4608-4611.
9. Busto, E., Richter, N., Grischek, B., & Kroutil, W. (2014). Biocontrolled formal inversion or retention of L- α -amino acids to enantiopure (*R*)-or (*S*)-Hydroxyacids. *Chemistry-A European Journal*, 20(35), 11225-11228.
10. Motta, P., Molla, G., Pollegioni, L., & Nardini, M. (2016). Structure-function relationships in L-amino acid deaminase, a flavoprotein belonging to a novel class of biotechnologically relevant enzymes. *Journal of Biological Chemistry*, 291(20), 10457-10475.
11. Pantaleone, D. P., Geller, A. M., & Taylor, P. P. (2001). Purification and characterization of an L-amino acid deaminase used to prepare unnatural amino acids. *Journal of Molecular Catalysis B: Enzymatic*, 11(4-6), 795-803.
12. Hossain, G. S., Li, J., Shin, H. D., Liu, L., Wang, M., Du, G., & Chen, J. (2014). Improved production of α -ketoglutaric acid (α -KG) by a *Bacillus subtilis* whole-cell biocatalyst *via* engineering of L-amino acid deaminase and deletion of the α -KG utilization pathway. *Journal of Biotechnology*, 187, 71-77.
13. Hinkes, S., Wuttke, A., Saupe, S. M., Ivanova, T., Wagner, S., Knörlein, A., & Steinmetzer, T. (2016). Optimization of cyclic plasmin inhibitors: From benzamidines to benzylamines. *Journal of Medicinal Chemistry*, 59(13), 6370-6386.
14. Saupe, S. M., Leubner, S., Betz, M., Klebe, G., & Steinmetzer, T. (2013).

- Development of new cyclic plasmin inhibitors with excellent potency and selectivity. *Journal of Medicinal Chemistry*, 56(3), 820-831.
15. Hou, Y., Hossain, G. S., Li, J., Shin, H. D., Liu, L., & Du, G. (2015). Production of phenylpyruvic acid from L-phenylalanine using an L-amino acid deaminase from *Proteus mirabilis*: comparison of enzymatic and whole-cell biotransformation approaches. *Applied Microbiology and Biotechnology*, 99(20), 8391-8402.
 16. Laskowski, R. A., & Swindells, M. B. (2011). LigPlot⁺: multiple ligand-protein interaction diagrams for drug discovery. *Journal of Chemical Information and Modeling*, 51 (10), 2778-2786.
 17. Hou, Y., Hossain, G. S., Li, J., Shin, H. D., Du, G., & Liu, L. (2016). Combination of phenylpyruvic acid (PPA) pathway engineering and molecular engineering of L-amino acid deaminase improves PPA production with an *Escherichia coli* whole-cell biocatalyst. *Applied Microbiology and Biotechnology*, 100(5), 2183-2191.
 18. Hossain, G. S., Li, J., Shin, H., Chen, R. R., Du, G., Liu, L., & Chen, J. (2014). Bioconversion of L-glutamic acid to α -ketoglutaric acid by an immobilized whole-cell biocatalyst expressing L-amino acid deaminase from *Proteus vulgaris*. *Journal of Biotechnology*, 169, 112-120.
 19. Hossain, G. S., Shin, H. D., Li, J., Wang, M., Du, G., Liu, L., & Chen, J. (2016). Integrating error-prone PCR and DNA shuffling as an effective molecular evolution strategy for the production of α -ketoglutaric acid by L-amino acid deaminase. *RSC Advances*, 6(52), 46149-46158.
 20. Hossain, G. S., Shin, H. D., Li, J., Du, G., Chen, J., & Liu, L. (2016). Transporter engineering and enzyme evolution for pyruvate production from D,L-alanine with a whole-cell biocatalyst expressing L-amino acid deaminase from *Proteus mirabilis*. *RSC Advances*, 6(86), 82676-82684.
 21. Hossain, G. S., Li, J., Shin, H. D., Du, G., Wang, M., Liu, L., & Chen, J. (2014). One-step biosynthesis of α -keto- γ -methylthiobutyric acid from L-methionine by an *Escherichia coli* whole-cell biocatalyst expressing an engineered L-amino acid deaminase from *Proteus vulgaris*. *PLoS one*, 9(12), e114291.
 22. Song, Y., Li, J., Shin, H. D., Du, G., Liu, L., & Chen, J. (2015). One-step biosynthesis of α -ketoisocaproate from L-leucine by an *Escherichia coli* whole-cell biocatalyst expressing an L-amino acid deaminase from *Proteus vulgaris*. *Scientific Reports*, 5, 12614.
 23. Li, R., Sakir, H. G., Li, J., Shin, H. D., Du, G., Chen, J., & Liu, L. (2017). Rational molecular engineering of L-amino acid deaminase for production of α -ketoisovaleric acid from L-valine by *Escherichia coli*. *RSC Advances*, 7(11), 6615-6621.
 24. Rosini, E., Melis, R., Molla, G., Tessaro, D., & Pollegioni, L. (2017). Deracemization and stereoinversion of α -amino acids by L-amino acid deaminase. *Advanced Synthesis & Catalysis*, 359(21), 3773-3781.
 25. Melis, R., Rosini, E., Pirillo, V., Pollegioni, L., & Molla, G. (2018). *In vitro* evolution of an L-amino acid deaminase active on L-1-naphthylalanine. Submitted.
 26. Caligiuri, A., D'Arrigo, P., Rosini, E., Tessaro, D., Molla, G., Servi, S., & Pollegioni, L. (2006). Enzymatic conversion of unnatural amino acids by yeast D-amino acid oxidase. *Advanced Synthesis & Catalysis*, 348(15), 2183-2190.
 27. Bornscheuer, U. T., Huisman, G. W., Kazlauskas, R. J., Lutz, S., Moore, J. C., &

- Robins, K. (2012). Engineering the third wave of biocatalysis. *Nature*, 485(7397), 185.
28. Reetz, M. T., Kahakeaw, D., & Lohmer, R. (2008). Addressing the numbers problem in directed evolution. *ChemBioChem*, 9(11), 1797-1804.
 29. Yasukawa, K., Nakano, S., & Asano, Y. (2014). Tailoring D-amino acid oxidase from the pig kidney to *R*-stereoselective amine oxidase and its use in the deracemization of α -methylbenzylamine. *Angewandte Chemie International Edition*, 53(17), 4428-4431.
 30. Trott, O., & Olson, A. J. (2010). AutoDock Vina: improving the speed and accuracy of docking with a new scoring function, efficient optimization, and multithreading. *Journal of Computational Chemistry*, 31(2), 455-461.

Sviluppo di un nuovo biocatalizzatore enantioselettivo di interesse biotecnologico attivo su L-amino acidi di interesse biotecnologico mediante un approccio di "semi-rational design" supportato da analisi computazionali.

La crescente domanda di composti chirali otticamente puri, da parte dell'industria farmaceutica e agrochimica per la sintesi di composti ad alto valore aggiunto, richiede lo sviluppo di processi biocatalitici. L'uso di enzimi come biocatalizzatori, si è rivelato un approccio concorrenziale, sia in termini di rese che di costi, rispetto agli approcci classici di sintesi organica asimmetrica. Gli enzimi, paragonati ai tradizionali catalizzatori inorganici possiedono diverse caratteristiche vantaggiose; ad esempio, una elevata chemo- regio-selettività ed efficienza catalitica in condizioni di reazione blande (pH neutro e temperatura ambiente). Queste caratteristiche rendono gli enzimi particolarmente adatti a catalizzare processi di deracemizzazione di miscele racemiche^{1,2}. Tuttavia, gli enzimi presenti in natura, raramente soddisfano i requisiti della biocatalisi industriale, in quanto le loro proprietà funzionali si sono evolute sotto una pressione selettiva legata unicamente alla loro funzione biologica. Pertanto, generalmente, gli enzimi naturali non presentano le caratteristiche ottimali per applicazioni biotecnologiche. Ciò comporta la necessità di ottimizzare i biocatalizzatori mediante tecniche di ingegneria proteica³.

Diversi protocolli per la produzione di L-amminoacidi otticamente puri sono stati messi a punto utilizzando come biocatalizzatore l'enzima D-amminoacido ossidasi (DAAO, wild-type o ingegnerizzato)^{4,5}. In linea di principio, la reazione speculare, catalizzata dalle L-amminoacido ossidasi (LAAO), potrebbe essere utilizzata per la produzione di D-amminoacidi puri e/o per la sintesi di α -chetoacidi, entrambi, composti di elevata importanza commerciale: questi composti sono utilizzati, ad esempio, come intermedi di reazione per la sintesi di prodotti farmaceutici, agrochimici e additivi alimentari^{6,7}. Tuttavia, la scarsa disponibilità di LAAO ricombinanti con un'ampia specificità di substrato, prodotte in forma , ne impedisce l'utilizzo su scala industriale¹. Una valida alternativa è rappresentata dalle L-amminoacido deaminasi (LAAD)^{8,9}, proteine di membrana isolate in batteri appartenenti al genere *Proteus*.

Le LAAD, come le LAAO, sono flavoenzimi che catalizzano la deaminazione ossidativa di L-amminoacidi con produzione del α -chetoacido corrispondente e ammonio. Tuttavia, a differenza di queste, in cui il cofattore ridotto viene riossidato dall'ossigeno molecolare con produzione di perossido di idrogeno, nelle LAAD gli elettroni vengono trasferiti dal FADH₂ a un accettore di elettroni di membrana. Di conseguenza, durante la catalisi, non si osserva la produzione di perossido di idrogeno: ciò consente di sovraesprimere l'enzima in forma ricombinante in procarioti (ad es. *Bacillus* e *E.coli*)^{8,10}.

Negli ultimi anni, diversi esempi di LAAD impiegate come biocatalizzatori enzimatici o a cellule intere sono stati riportati in letteratura, dimostrando la fattibilità di questo approccio^{9,11-14}. Inoltre, la recente caratterizzazione funzionale e strutturale della LAAD ricombinante isolata da *P. myxofaciens* (PmaLAAD)¹⁰ ha aperto la strada al suo sfruttamento in biocatalisi enantioselettiva e alla sua ottimizzazione mediante ingegneria proteica.

Il presente progetto di dottorato, si è focalizzato: 1) sullo sviluppo di processi di biocatalisi stereoselettivi per la produzione di D-amminoacidi e α -chetoacidi sfruttando come biocatalizzatore l'enzima PmaLAAD wild-type; 2) sull'ottimizzazione dell'enzima PmaLAAD mediante un approccio di "semi-rational design", finalizzato alla produzione di varianti con attività enzimatica migliorata sul substrato L-1-naftilalanina (L-1-Nal); 3) sull'applicazione di strategie alternative di ingegneria proteica mirate ad implementare l'attività dell'enzima su substrati di interesse biotecnologico.

La prima parte di questo progetto si è concentrata sullo sviluppo e ottimizzazione di un nuovo processo biocatalitico per la produzione di D-amminoacidi otticamente puri e α -chetoacidi di rilevanza farmaceutica e biotecnologica, utilizzando l'enzima PmaLAAD purificato come biocatalizzatore. Questo approccio, ha permesso di superare alcuni problemi dell'utilizzo del biocatalizzatore come cellule intere come, ad esempio, il ridotto trasferimento di massa dovuto alla presenza della membrana cellulare (rilevante per biotrasformazioni di substrati sintetici, per i quali non sono presenti specifici sistemi di trasporto) e il consumo dei prodotti desiderati (o la formazione di prodotti indesiderati) durante la biocatalisi causati dalla presenza di attività enzimatiche endogene.

Sfruttando l'ampia specificità di substrato dell'enzima PmaLAAD ricombinante, attivo su diversi L-amminoacidi (sia naturali, che di sintesi)¹⁰, abbiamo utilizzato questo biocatalizzatore per la catalisi di diverse biotrasformazioni enantioselettive¹⁵. Ad esempio, PmaLAAD è stata utilizzata per la produzione di α -chetoacidi puri a partire dai corrispondenti L-amminoacidi (ad es. fenilpiruvato da L-fenilalanina o α -chetoisocaproato da L-leucina). Inoltre, PmaLAAD è stata impiegata per la produzione di D-amminoacidi otticamente puri attraverso processi di deracemizzazione di soluzioni racemiche di D,L-amminoacidi o per catalizzare la completa stereoinversione di un L-amminoacido con produzione del corrispondente D-enantiomero (ad es., è stato sintetizzato a partire dal suo L-enantiomero il composto D-4-nitrofenilalanina, utilizzato per la produzione di farmaci anti-fibrinolitici e inibitori della plasmina^{16,17}). L'uso di PmaLAAD come preparazione enzimatica purificata, ha consentito mettere a punto reazioni di bioconversione di diversi substrati (es., L-Phe, L-Leu e L-Met) più rapide, ottenendo rese di conversione più elevate (> 99%)¹⁵ rispetto ai sistemi di biocatalisi a cellule intere riportate in letteratura^{12,18-20}.

L'utilizzo di PmaLAAD, che non produce perossido di idrogeno durante la catalisi, consentirà di evitare 'l'aggiunta di sistemi di eliminazione delle specie ROS (ad es., catalasi). Ciò ha facilitato il recupero del prodotto e determinando un'ulteriore riduzione dei costi complessivi di biotrasformazione.

Recentemente è stata risolta la struttura 3D di PmaLAAD¹⁰. La conoscenza dettagliata della struttura terziaria ha consentito la progettazione e produzione di varianti enzimatiche di PmaLAAD mediante ingegneria proteica semi-razionale adatte per la messa a punto di bioconversioni del substrato di interesse biotecnologico L-1-naftilalanina (L-1-Nal).

I residui coinvolti nella specificità di substrato, identificati mediante analisi di docking molecolare, sono stati sottoposti a site-saturation mutagenesi (singolarmente o in combinazione). Tutte le varianti selezionate mediante screening di attività per il substrato di interesse, mostrano un aumento dell'efficienza catalitica su D,L-1-Nal (rispetto all'enzima wild-type) e una significativa riduzione della stessa sui rimanenti substrati analizzati. La variante più interessante, F318A/V412A/V438P-PmaLAAD, è in grado di deracemizzare una miscela di D,L-

1-Nal con una velocità 7.5 volte superiore rispetto all'enzima wild-type. Ciò ha consentito di sviluppare un processo di biotrasformazione efficiente per la produzione dell' enantiomero D o del corrispondente α -chetoacido (non ancora disponibile in commercio). In quest'ultimo caso, PmaLAAD deve essere utilizzata in combinazione con la variante M213G della D-amminoacido ossidasi.

Al fine di ottenere varianti di PmaLAAD aventi una maggiore diversificazione della specificità di substrato (ad es. per ottenere varianti attive su L-Asp, L-tert-Leu e L-penicillamina), sono stati valutati, in forma preliminare, alcuni approcci di ingegneria proteica in grado di introdurre diverse mutazioni contemporaneamente in PmaLAAD. Tali approcci sono basati su un esame approfondito della relazione struttura/funzione nell'enzima PmaLAAD al fine di produrre delle librerie di varianti 'smaller but smarter', cioè aventi una probabilità maggiore di contenere varianti enzimatiche desiderate.

Gli approcci utilizzati sono i seguenti:

1) la conversione del sito attivo di PmaLAAD (LAAD di tipo I) in quello dell'enzima pvLAAD (LAAD di tipo II), il quale possiede una specificità di substrato differente nonostante l'elevata omologia di sequenza tra le due proteine prese in esame; 2) la produzione di un LAAD 'generalista' (cioè avente una specificità di substrato ampia) basata sulla sequenza di una putativa LAAD "ancestrale" e 3) l'introduzione combinatoriale di un numero definito di mutazioni in un numero ristretto di posizioni aminoacidiche (mutagenesi "fattoriale" sito-specifica). I risultati preliminari ottenuti hanno permesso di comprendere le potenzialità e i limiti degli approcci considerati. In particolare, grazie anche ad analisi di docking molecolare, è stata evidenziata la complessità di ottenere varianti enzimatiche attive su substrati di piccole dimensioni (es., L-Ala, L-Ser o L-penicillamina). Infatti, il sito attivo dell'enzima wild-type è definito da residui voluminosi (ad es., Phe318, Trp439 e Gln100). La sostituzione di un numero molto piccolo di residui (da 1 a 3) non consente di ottenere una riduzione significativa del volume della tasca idrofobica del sito attivo, mentre, l'incremento dello stesso è ottenibile più efficacemente.

In conclusione, l'attività di ricerca svolta durante questo progetto di dottorato ha consentito la produzione di diverse varianti di PmaLAAD più efficienti sul substrato

sintetico di interesse biotecnologico L-1-Nal e la messa a punto di protocolli di biocatalisi basati sia sull'enzima wild-type sia su diverse varianti migliorate. PmaLAAD rappresenta, quindi, una valida un'alternativa rispetto alle LAAO canoniche come biocatalizzatore per la produzione di D-amminoacidi otticamente puri o α -chetoacidi. La caratterizzazione biochimica delle varianti prodotte ha consentito di comprendere meglio il rapporto struttura funzione in questo enzima (e negli enzimi omologhi) e di porre le basi per ulteriori fasi di evoluzione *in vitro* delle proprietà catalitiche di PmaLAAD.

References

1. Pollegioni, L., Motta, P., & Molla, G. (2013). L-Amino acid oxidase as biocatalyst: a dream too far?. *Applied Microbiology and Biotechnology*, 97(21), 9323-9341.
2. Turner, N. J. (2004). Enzyme catalysed deracemisation and dynamic kinetic resolution reactions. *Current Opinion in Chemical Biology*, 8(2), 114-119.
3. Steiner, K., & Schwab, H. (2012). Recent advances in rational approaches for enzyme engineering. *Computational and Structural Biotechnology Journal*, 2(3), e201209010.
4. Pollegioni, L., & Molla, G. (2011). New biotech applications from evolved D-amino acid oxidases. *Trends in Biotechnology*, 29(6), 276-283.
5. Pollegioni, L., Sacchi, S., Caldinelli, L., Boselli, A., Pilone, M. S., Piubelli, L., & Molla, G. (2007). Engineering the properties of D-amino acid oxidases by a rational and a directed evolution approach. *Current Protein and Peptide Science*, 8(6), 600-618.
6. Song, Y., Li, J., Shin, H. D., Liu, L., Du, G., & Chen, J. (2016). Biotechnological production of alpha-keto acids: current status and perspectives. *Bioresource Technology*, 219, 716-724.
7. Gao, X., Ma, Q., & Zhu, H. (2015). Distribution, industrial applications, and enzymatic synthesis of D-amino acids. *Applied Microbiology and Biotechnology*, 99(8), 3341-3349.
8. Pantaleone, D. P., Geller, A. M., & Taylor, P. P. (2001). Purification and characterization of an L-amino acid deaminase used to prepare unnatural amino acids. *Journal of Molecular Catalysis B: Enzymatic*, 11(4-6), 795-803.
9. Molla, G., Melis, R., & Pollegioni, L. (2017). Breaking the mirror: L-Amino acid deaminase, a novel stereoselective biocatalyst. *Biotechnology Advances*, 35(6), 657-668.
10. Motta, P., Molla, G., Pollegioni, L., & Nardini, M. (2016). Structure-function relationships in L-amino acid deaminase, a flavoprotein belonging to a novel class of biotechnologically relevant enzymes. *Journal of Biological Chemistry*, jbc-M115.
11. Alexandre, F. R., Pantaleone, D. P., Taylor, P. P., Fotheringham, I. G., Ager, D. J., & Turner, N. J. (2002). Amine-boranes: effective reducing agents for the deracemisation of D,L-amino acids using L-amino acid oxidase from *Proteus myxofaciens*. *Tetrahedron Letters*, 43(4), 707-710.
12. Hou, Y., Hossain, G. S., Li, J., Shin, H. D., Liu, L., Du, G., & Chen, J. (2016). Two-Step production of phenylpyruvic acid from L-phenylalanine by growing and resting cells of engineered *Escherichia coli*: process optimization and kinetics modeling. *PloS one*, 11(11), e0166457.
13. Parmeggiani, F., Lovelock, S. L., Weise, N. J., Ahmed, S. T., & Turner, N. J. (2015). Synthesis of d-and L-phenylalanine derivatives by phenylalanine ammonia lyases: a multienzymatic cascade process. *Angewandte Chemie International Edition*, 54(15), 4608-4611.
14. Busto, E., Richter, N., Grischek, B., & Kroutil, W. (2014). Biocontrolled formal inversion or retention of L- α -amino acids to enantiopure (*R*)-or (*S*)-Hydroxyacids. *Chemistry-A European Journal*, 20(35), 11225-11228.

15. Rosini, E., Melis, R., Molla, G., Tessaro, D., & Pollegioni, L. (2017). Deracemization and stereoinversion of α -amino acids by L-amino acid deaminase. *Advanced Synthesis & Catalysis*, 359(21), 3773-3781.
16. Hinkes, S., Wuttke, A., Saupe, S. M., Ivanova, T., Wagner, S., Knorlein, A., & Steinmetzer, T. (2016). Optimization of cyclic plasmin inhibitors: from benzamidines to benzylamines. *Journal of Medicinal Chemistry*, 59(13), 6370-6386.
17. Saupe, S. M., Leubner, S., Betz, M., Klebe, G., & Steinmetzer, T. (2013). Development of new cyclic plasmin inhibitors with excellent potency and selectivity. *Journal of Medicinal Chemistry*, 56(3), 820-831.
18. Hou, Y., Hossain, G. S., Li, J., Shin, H. D., Liu, L., & Du, G. (2015). Production of phenylpyruvic acid from L-phenylalanine using an L-amino acid deaminase from *Proteus mirabilis*: comparison of enzymatic and whole-cell biotransformation approaches. *Applied Microbiology and Biotechnology*, 99(20), 8391-8402.
19. Hossain, G. S., Li, J., Shin, H. D., Du, G., Wang, M., Liu, L., & Chen, J. (2014). One-step biosynthesis of α -keto- γ -methylthiobutyric acid from L-methionine by an *Escherichia coli* whole-cell biocatalyst expressing an engineered L-amino acid deaminase from *Proteus vulgaris*. *PloS one*, 9(12), e114291.
20. Li, R., Sakir, H. G., Li, J., Shin, H. D., Du, G., Chen, J., & Liu, L. (2017). Rational molecular engineering of L-amino acid deaminase for production of α -ketoisovaleric acid from L-valine by *Escherichia coli*. *RSC Advances*, 7(11), 6615-6621.